

## CONTENTS

List of Boxes	xiii	
Preface	xv	
Contents of <i>Modern Classical Physics</i> , volumes 1-5	xxi	
<b>19</b>	<b>Magnetohydrodynamics</b>	<b>943</b>
19.1	Overview	943
19.2	Basic Equations of MHD	944
	19.2.1 Maxwell's Equations in the MHD Approximation	946
	19.2.2 Momentum and Energy Conservation	950
	19.2.3 Boundary Conditions	953
	19.2.4 Magnetic Field and Vorticity	957
19.3	Magnetostatic Equilibria	958
	19.3.1 Controlled Thermonuclear Fusion	958
	19.3.2 Z-Pinch	960
	19.3.3 $\Theta$ -Pinch	962
	19.3.4 Tokamak	963
19.4	Hydromagnetic Flows	965
19.5	Stability of Magnetostatic Equilibria	971
	19.5.1 Linear Perturbation Theory	971
	19.5.2 Z-Pinch: Sausage and Kink Instabilities	975
	19.5.3 The $\Theta$ -Pinch and Its Toroidal Analog; Flute Instability; Motivation for Tokamak	978
	19.5.4 Energy Principle and Virial Theorems	980
19.6	Dynamos and Reconnection of Magnetic Field Lines	984
	19.6.1 Cowling's Theorem	984
	19.6.2 Kinematic Dynamos	985
	19.6.3 Magnetic Reconnection	986

---

**T2** Track Two; see page xvi

- 19.7 Magnetosonic Waves and the Scattering of Cosmic Rays 988
  - 19.7.1 Cosmic Rays 988
  - 19.7.2 Magnetosonic Dispersion Relation 989
  - 19.7.3 Scattering of Cosmic Rays by Alfvén Waves 992
- Bibliographic Note 993

## **PART VI PLASMA PHYSICS 995**

---

- 20 The Particle Kinetics of Plasma 997**
  - 20.1 Overview 997
  - 20.2 Examples of Plasmas and Their Density-Temperature Regimes 998
    - 20.2.1 Ionization Boundary 998
    - 20.2.2 Degeneracy Boundary 1000
    - 20.2.3 Relativistic Boundary 1000
    - 20.2.4 Pair-Production Boundary 1001
    - 20.2.5 Examples of Natural and Human-Made Plasmas 1001
  - 20.3 Collective Effects in Plasmas—Debye Shielding and Plasma Oscillations 1003
    - 20.3.1 Debye Shielding 1003
    - 20.3.2 Collective Behavior 1004
    - 20.3.3 Plasma Oscillations and Plasma Frequency 1005
  - 20.4 Coulomb Collisions 1006
    - 20.4.1 Collision Frequency 1006
    - 20.4.2 The Coulomb Logarithm 1008
    - 20.4.3 Thermal Equilibration Rates in a Plasma 1010
    - 20.4.4 Discussion 1012
  - 20.5 Transport Coefficients 1015
    - 20.5.1 Coulomb Collisions 1015
    - 20.5.2 Anomalous Resistivity and Anomalous Equilibration 1016
  - 20.6 Magnetic Field 1019
    - 20.6.1 Cyclotron Frequency and Larmor Radius 1019
    - 20.6.2 Validity of the Fluid Approximation 1020
    - 20.6.3 Conductivity Tensor 1022
  - 20.7 Particle Motion and Adiabatic Invariants 1024
    - 20.7.1 Homogeneous, Time-Independent Magnetic Field and No Electric Field 1025
    - 20.7.2 Homogeneous, Time-Independent Electric and Magnetic Fields 1025
    - 20.7.3 Inhomogeneous, Time-Independent Magnetic Field 1026
    - 20.7.4 A Slowly Time-Varying Magnetic Field 1029
    - 20.7.5 Failure of Adiabatic Invariants; Chaotic Orbits 1030
  - Bibliographic Note 1032

<b>21</b>	<b>Waves in Cold Plasmas: Two-Fluid Formalism</b>	<b>1033</b>	
21.1	Overview	1033	
21.2	Dielectric Tensor, Wave Equation, and General Dispersion Relation	1035	
21.3	Two-Fluid Formalism	1037	
21.4	Wave Modes in an Unmagnetized Plasma	1040	
	21.4.1 Dielectric Tensor and Dispersion Relation for a Cold, Unmagnetized Plasma	1040	
	21.4.2 Plasma Electromagnetic Modes	1042	
	21.4.3 Langmuir Waves and Ion-Acoustic Waves in Warm Plasmas	1044	
	21.4.4 Cutoffs and Resonances	1049	
21.5	Wave Modes in a Cold, Magnetized Plasma	1050	
	21.5.1 Dielectric Tensor and Dispersion Relation	1050	
	21.5.2 Parallel Propagation	1052	
	21.5.3 Perpendicular Propagation	1057	
	21.5.4 Propagation of Radio Waves in the Ionosphere; Magnetoionic Theory	1058	
	21.5.5 CMA Diagram for Wave Modes in a Cold, Magnetized Plasma	1062	
21.6	Two-Stream Instability	1065	
	Bibliographic Note	1068	
<b>22</b>	<b>Kinetic Theory of Warm Plasmas</b>	<b>1069</b>	
22.1	Overview	1069	
22.2	Basic Concepts of Kinetic Theory and Its Relationship to Two-Fluid Theory	1070	
	22.2.1 Distribution Function and Vlasov Equation	1070	
	22.2.2 Relation of Kinetic Theory to Two-Fluid Theory	1073	
	22.2.3 Jeans' Theorem	1074	
22.3	Electrostatic Waves in an Unmagnetized Plasma: Landau Damping	1077	
	22.3.1 Formal Dispersion Relation	1077	
	22.3.2 Two-Stream Instability	1079	
	22.3.3 The Landau Contour	1080	
	22.3.4 Dispersion Relation for Weakly Damped or Growing Waves	1085	
	22.3.5 Langmuir Waves and Their Landau Damping	1086	
	22.3.6 Ion-Acoustic Waves and Conditions for Their Landau Damping to Be Weak	1088	
22.4	Stability of Electrostatic Waves in Unmagnetized Plasmas	1090	
	22.4.1 Nyquist's Method	1091	
	22.4.2 Penrose's Instability Criterion	1091	
22.5	Particle Trapping	1098	
22.6	<i>N</i> -Particle Distribution Function	1102	T2
	22.6.1 BBGKY Hierarchy	1103	T2
	22.6.2 Two-Point Correlation Function	1104	T2
	22.6.3 Coulomb Correction to Plasma Pressure	1107	T2
	Bibliographic Note	1108	

<b>23</b>	<b>Nonlinear Dynamics of Plasmas</b>	<b>1111</b>
23.1	Overview	1111
23.2	Quasilinear Theory in Classical Language	1113
	23.2.1 Classical Derivation of the Theory	1113
	23.2.2 Summary of Quasilinear Theory	1120
	23.2.3 Conservation Laws	1121
	23.2.4 Generalization to 3 Dimensions	1122
23.3	Quasilinear Theory in Quantum Mechanical Language	1123
	23.3.1 Plasmon Occupation Number $\eta$	1123
	23.3.2 Evolution of $\eta$ for Plasmons via Interaction with Electrons	1124
	23.3.3 Evolution of $f$ for Electrons via Interaction with Plasmons	1129
	23.3.4 Emission of Plasmons by Particles in the Presence of a Magnetic Field	1131
	23.3.5 Relationship between Classical and Quantum Mechanical Formalisms	1131
	23.3.6 Evolution of $\eta$ via Three-Wave Mixing	1132
23.4	Quasilinear Evolution of Unstable Distribution Functions—A Bump in the Tail	1136
	23.4.1 Instability of Streaming Cosmic Rays	1138
23.5	Parametric Instabilities; Laser Fusion	1140
23.6	Solitons and Collisionless Shock Waves	1142
	Bibliographic Note	1149
<b>App. A</b>	<b>Evolution of Vorticity</b>	<b>1151</b>
14.2	Vorticity, Circulation, and Their Evolution	1151
	14.2.1 Vorticity Evolution	1153
	14.2.2 Barotropic, Inviscid, Compressible Flows: Vortex Lines Frozen into Fluid	1156
<b>App. B</b>	<b>Geometric Optics</b>	<b>1159</b>
7.2	Waves in a Homogeneous Medium	1159
	7.2.1 Monochromatic Plane Waves; Dispersion Relation	1159
	7.2.2 Wave Packets	1161
7.3	Waves in an Inhomogeneous, Time-Varying Medium: The Eikonal Approximation and Geometric Optics	1164
	7.3.1 Geometric Optics for a Prototypical Wave Equation	1165
	7.3.2 Connection of Geometric Optics to Quantum Theory	1169
	7.3.3 Geometric Optics for a General Wave	1173
	7.3.4 Examples of Geometric-Optics Wave Propagation	1175
	7.3.5 Relation to Wave Packets; Limitations of the Eikonal Approximation and Geometric Optics	1176
	7.3.6 Fermat's Principle	1178

<b>App. C</b>	<b>Distribution Function and Mean Occupation Number</b>	<b>1183</b>
3.2	Phase Space and Distribution Function	1183
3.2.1	Newtonian Number Density in Phase Space, $\mathcal{N}$	1183
3.2.3	Distribution Function $f(\mathbf{x}, \mathbf{v}, t)$ for Particles in a Plasma	1185
3.2.5	Mean Occupation Number $\eta$	1185
	References	1189
	Name Index	1193
	Subject Index	1195
	Contents of the Unified Work, <i>Modern Classical Physics</i>	1203
	Preface to <i>Modern Classical Physics</i>	1211
	Acknowledgments for <i>Modern Classical Physics</i>	1219

## Magnetohydrodynamics

... it is only the plasma itself which does not 'understand' how beautiful the theories are and absolutely refuses to obey them.

HANNES ALFVÉN (1970)

### 19.1 Overview

19.1

In preceding chapters we have described the consequences of incorporating viscosity and thermal conductivity into the description of a fluid. We now turn to our final embellishment of fluid mechanics, in which the fluid is electrically conducting and moves in a magnetic field. The study of flows of this type is known as *magnetohydrodynamics*, or MHD for short. In our discussion, we eschew full generality and with one exception just use the basic Euler equation (no viscosity, no heat diffusion, etc.) augmented by magnetic terms. This approach suffices to highlight peculiarly magnetic effects and is adequate for many applications.

The simplest example of an electrically conducting fluid is a liquid metal, for example, mercury or liquid sodium. However, the major application of MHD is in plasma physics—discussed in Part VI. (A plasma is a hot, ionized gas containing free electrons and ions.) It is by no means obvious that plasmas can be regarded as fluids, since the mean free paths for Coulomb-force collisions between a plasma's electrons and ions are macroscopically long. However, as we shall learn in Sec. 20.5, collective interactions between large numbers of plasma particles can isotropize the particles' velocity distributions in some local mean reference frame, thereby making it sensible to describe the plasma macroscopically by a mean density, velocity, and pressure. These mean quantities can then be shown to obey the same conservation laws of mass, momentum, and energy as we derived for fluids in Chap. 13. As a result, a fluid description of a plasma is often reasonably accurate. We defer to Part VI further discussion of this point, asking the reader to take it on trust for the moment. In MHD, we also implicitly assume that the average velocity of the ions is nearly the same as the average velocity of the electrons. This is usually a good approximation; if it were not so, then the plasma would carry an unreasonably large current density.

Two serious technological applications of MHD may become very important in the future. In the first, strong magnetic fields are used to confine rings or columns of hot plasma that (it is hoped) will be held in place long enough for thermonuclear fusion to occur and for net power to be generated. In the second, which is directed toward a

943

### BOX 19.1. READERS' GUIDE

- This chapter relies heavily on Chap. 13 and somewhat on the treatment of vorticity transport in Sec. 14.2.
- Part VI, Plasma Physics (Chaps. 20–23), relies heavily on this chapter.

similar goal, liquid metals or plasmas are driven through a magnetic field to generate electricity. The study of magnetohydrodynamics is also motivated by its widespread application to the description of space (in the solar system) and astrophysical plasmas (beyond the solar system). We illustrate the principles of MHD using examples drawn from all these areas.

After deriving the basic equations of MHD (Sec. 19.2), we elucidate magnetostatic (also called “hydromagnetic”) equilibria by describing a *tokamak* (Sec. 19.3). This is currently the most popular scheme for the magnetic confinement of hot plasma. In our second application (Sec. 19.4) we describe the flow of conducting liquid metals or plasma along magnetized ducts and outline its potential as a practical means of electrical power generation and spacecraft propulsion. We then return to the question of magnetostatic confinement of hot plasma and focus on the stability of equilibria (Sec. 19.5). This issue of stability has occupied a central place in our development of fluid mechanics, and it will not come as a surprise to learn that it has dominated research on thermonuclear fusion in plasmas. When a magnetic field plays a role in the equilibrium (e.g., for magnetic confinement of a plasma), the field also makes possible new modes of oscillation, and some of these MHD modes can be unstable to exponential growth. Many magnetic-confinement geometries exhibit such instabilities. We demonstrate this qualitatively by considering the physical action of the magnetic field, and also formally by using variational methods.

In Sec. 19.6, we turn to a geophysical problem, the origin of Earth’s magnetic field. It is generally believed that complex fluid motions in Earth’s liquid core are responsible for regenerating the field through dynamo action. We use a simple model to illustrate this process.

When magnetic forces are added to fluid mechanics, a new class of waves, called magnetosonic waves, can propagate. We conclude our discussion of MHD in Sec. 19.7 by deriving the properties of these wave modes in a homogeneous plasma and discussing how they control the propagation of cosmic rays in the interplanetary and interstellar media.

As in previous chapters, we encourage our readers to view films; on magnetohydrodynamics, for example, Shercliff (1965).

## 19.2 19.2 Basic Equations of MHD

The equations of MHD describe the motion of a conducting fluid in a magnetic field. This fluid is usually either a liquid metal or a plasma. In both cases, the conductivity,

strictly speaking, should be regarded as a tensor (Sec. 20.6.3) if the electrons' cyclotron frequency (Sec. 20.6.1) exceeds their collision frequency (the inverse of the mean time between collisions; Sec. 20.4.1). (If there are several collisions per cyclotron orbit, then the influence of the magnetic field on the transport coefficients will be minimal.) However, to keep the mathematics simple, we treat the conductivity as a constant scalar,  $\kappa_e$ . In fact, it turns out that for many of our applications, it is adequate to take the conductivity as infinite, and it does not matter whether that infinity is a scalar or a tensor!

Two key physical effects occur in MHD, and understanding them well is key to developing physical intuition. The first effect arises when a good conductor moves into a magnetic field (Fig. 19.1a). Electric current is induced in the conductor, which, by Lenz's law, creates its own magnetic field. This induced magnetic field tends to cancel the original, externally supported field, thereby in effect excluding the magnetic field lines from the conductor. Conversely, when the magnetic field penetrates the conductor and the conductor is moved out of the field, the induced field reinforces the applied field. The net result is that the lines of force appear to be dragged along with the conductor—they “go with the flow.” Naturally, if the conductor is a fluid with complex motions, the ensuing magnetic field distribution can become quite complex, and the current builds up until its growth is balanced by Ohmic dissipation.

The second key effect is dynamical. When currents are induced by a motion of a conducting fluid through a magnetic field, a Lorentz (or  $\mathbf{j} \times \mathbf{B}$ ) force acts on the fluid and modifies its motion (Fig. 19.1b). In MHD, the motion modifies the field, and the field, in turn, reacts back and modifies the motion. This behavior makes the theory highly nonlinear.

Before deriving the governing equations of MHD, we should consider the choice of primary variables. In electromagnetic theory, we specify the spatial and temporal variation of either the electromagnetic field or its source, the electric charge density and current density. One choice is computable (at least in principle) from the other

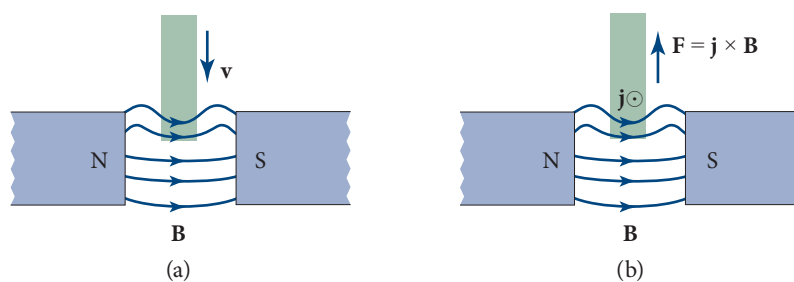


**FIGURE 19.1** The two key physical effects that occur in MHD. (a) A moving conductor modifies the magnetic field by dragging the field lines with it. When the conductivity is infinite, the field lines are frozen in the moving conductor. (b) When electric current, flowing in the conductor, crosses magnetic field lines, a Lorentz force is generated that accelerates the fluid.

two key physical effects in MHD

using Maxwell's equations, augmented by suitable boundary conditions. So it is with MHD, and the choice depends on convenience. It turns out that for the majority of applications, it is most instructive to deal with the magnetic field as primary, and to use Maxwell's equations

in MHD the magnetic field is the primary variable

Maxwell's equations

$$\nabla \cdot \mathbf{E} = \frac{\rho_e}{\epsilon_0}, \quad (19.1a)$$

$$\nabla \cdot \mathbf{B} = 0, \quad (19.1b)$$

$$\nabla \times \mathbf{E} = -\frac{\partial \mathbf{B}}{\partial t}, \quad (19.1c)$$

$$\nabla \times \mathbf{B} = \mu_0 \mathbf{j} + \mu_0 \epsilon_0 \frac{\partial \mathbf{E}}{\partial t} \quad (19.1d)$$

to express the electric field  $\mathbf{E}$ , the current density  $\mathbf{j}$ , and the charge density  $\rho_e$  in terms of the magnetic field (next subsection).

### 19.2.1 19.2.1 Maxwell's Equations in the MHD Approximation

As normally formulated, Ohm's law is valid only in the rest frame of the conductor. In particular, for a conducting fluid, Ohm's law relates the current density  $\mathbf{j}'$  measured in the fluid's local rest frame to the electric field  $\mathbf{E}'$  measured there:

$$\mathbf{j}' = \kappa_e \mathbf{E}', \quad (19.2)$$

where  $\kappa_e$  is the scalar electric conductivity. Because the fluid is generally accelerated,  $d\mathbf{v}/dt \neq 0$ , its local rest frame is generally not inertial. Since it would produce a terrible headache to have to transform time and again from some inertial frame to the continually changing local rest frame when applying Ohm's law, it is preferable to reformulate Ohm's law in terms of the fields  $\mathbf{E}$ ,  $\mathbf{B}$ , and  $\mathbf{j}$  measured in an inertial frame. To facilitate this (and for completeness), we explore the frame dependence of all our electromagnetic quantities  $\mathbf{E}$ ,  $\mathbf{B}$ ,  $\mathbf{j}$ , and  $\rho_e$ .

Throughout our development of magnetohydrodynamics, we assume that the fluid moves with a nonrelativistic speed  $v \ll c$  relative to our chosen reference frame. We can then express the rest-frame electric field in terms of the inertial-frame electric and magnetic fields as

$$\mathbf{E}' = \mathbf{E} + \mathbf{v} \times \mathbf{B}; \quad E' = |\mathbf{E}'| \ll E, \quad \text{so } \mathbf{E} \simeq -\mathbf{v} \times \mathbf{B}. \quad (19.3a)$$

In the first equation we have set the Lorentz factor  $\gamma \equiv 1/\sqrt{1 - v^2/c^2}$  to unity, consistent with our nonrelativistic approximation. The second equation follows from the high conductivity of the fluid, which guarantees that current will quickly flow in whatever manner it must to annihilate any electric field  $\mathbf{E}'$  that might be formed in the fluid's local rest frame. By contrast with the extreme frame dependence (19.3a) of the electric

field, the magnetic field is essentially the same in the fluid's local rest frame as in the laboratory. More specifically, the analog of Eq. (19.3a) is  $\mathbf{B}' = \mathbf{B} - (\mathbf{v}/c^2) \times \mathbf{E}$ ; and since  $E \sim vB$ , the second term is of magnitude  $(v/c)^2 B$ , which is negligible, giving

$$\mathbf{B}' \simeq \mathbf{B}. \quad (19.3b)$$

Because  $\mathbf{E}$  is highly frame dependent, so is its divergence, the electric charge density  $\rho_e$ . In the laboratory frame, where  $E \sim vB$ , Gauss's and Ampère's laws [Eqs. (19.1a,d)] imply that  $\rho_e \sim \epsilon_0 v B/L \sim (v/c^2) j$ , where  $L$  is the lengthscale on which  $\mathbf{E}$  and  $\mathbf{B}$  vary; and the relation  $E' \ll E$  with Gauss's law implies  $|\rho_e'| \ll |\rho_e|$ :

$$\rho_e \sim j v/c^2, \quad |\rho_e'| \ll |\rho_e|. \quad (19.3c)$$

By transforming the current density between frames and approximating  $\gamma \simeq 1$ , we obtain  $\mathbf{j}' = \mathbf{j} + \rho_e \mathbf{v} = \mathbf{j} + O(v/c)^2 j$ ; so in the nonrelativistic limit (first order in  $v/c$ ) we can ignore the charge density and write

$$\mathbf{j}' = \mathbf{j}. \quad (19.3d)$$

To recapitulate, in nonrelativistic magnetohydrodynamic flows, the magnetic field and current density are frame independent up to fractional corrections of order  $(v/c)^2$ , while the electric field and charge density are highly frame dependent and are generally small in the sense that  $E/c \sim (v/c)B \ll B$  and  $\rho_e \sim (v/c^2)j \ll j/c$  [in Gaussian cgs units we have  $E \sim (v/c)B \ll B$  and  $\rho_e c \sim (v/c)j \ll j$ ].

Combining Eqs. (19.2), (19.3a), and (19.3d), we obtain the nonrelativistic form of Ohm's law in terms of quantities measured in our chosen inertial, laboratory frame:

$$\mathbf{j} = \kappa_e (\mathbf{E} + \mathbf{v} \times \mathbf{B}). \quad (19.4)$$

We are now ready to derive explicit equations for the (inertial-frame) electric field and current density in terms of the (inertial-frame) magnetic field. In our derivation, we denote by  $L$  the lengthscale on which the magnetic field changes.

We begin with Ampère's law written as  $\nabla \times \mathbf{B} - \mu_0 \mathbf{j} = \mu_0 \epsilon_0 \partial \mathbf{E} / \partial t = (1/c^2) \partial \mathbf{E} / \partial t$ , and we notice that the time derivative of  $\mathbf{E}$  is of order  $E v/L \sim B v^2/L$  (since  $E \sim vB$ ). Therefore, the right-hand side is  $O[B v^2/(c^2 L)]$  and thus can be neglected compared to the  $O(B/L)$  term on the left, yielding:

$$\mathbf{j} = \frac{1}{\mu_0} \nabla \times \mathbf{B}. \quad (19.5a)$$

We next insert this expression for  $\mathbf{j}$  into the inertial-frame Ohm's law (19.4), thereby obtaining

$$\mathbf{E} = -\mathbf{v} \times \mathbf{B} + \frac{1}{\kappa_e \mu_0} \nabla \times \mathbf{B}. \quad (19.5b)$$

in MHD, magnetic field and current density are approximately frame independent; electric field and charge density are small and frame dependent

Ohm's law

current density in terms of magnetic field

electric field in terms of magnetic field

If we happen to be interested in the charge density (which is rare in MHD), we can compute it by taking the divergence of this electric field:

charge density in terms of magnetic field

$$\rho_e = -\epsilon_0 \nabla \cdot (\mathbf{v} \times \mathbf{B}). \quad (19.5c)$$

Equations (19.5) express all the secondary electromagnetic variables in terms of our primary one,  $\mathbf{B}$ . This has been possible because of the high electric conductivity  $\kappa_e$  and our choice to confine ourselves to nonrelativistic (low-velocity) situations; it would not be possible otherwise.

We next derive an evolution law for the magnetic field by taking the curl of Eq. (19.5b), using Maxwell's equation  $\nabla \times \mathbf{E} = -\partial \mathbf{B} / \partial t$  and the vector identity  $\nabla \times (\nabla \times \mathbf{B}) = \nabla(\nabla \cdot \mathbf{B}) - \nabla^2 \mathbf{B}$ , and using  $\nabla \cdot \mathbf{B} = 0$ . The result is

evolution law for magnetic field

$$\frac{\partial \mathbf{B}}{\partial t} = \nabla \times (\mathbf{v} \times \mathbf{B}) + \left( \frac{1}{\mu_0 \kappa_e} \right) \nabla^2 \mathbf{B}, \quad (19.6)$$

which, using Eqs. (14.4) and (14.5) with  $\boldsymbol{\omega}$  replaced by  $\mathbf{B}$ , can also be written as

$$\frac{D\mathbf{B}}{Dt} = -\mathbf{B} \nabla \cdot \mathbf{v} + \left( \frac{1}{\mu_0 \kappa_e} \right) \nabla^2 \mathbf{B}, \quad (19.7)$$

where  $D/Dt$  is the fluid derivative defined in Eq. (14.5). When the flow is incompressible (as it often will be), the  $\nabla \cdot \mathbf{v}$  term vanishes.

Equation (19.6)—or equivalently, Eq. (19.7)—is called the *induction equation* and describes the temporal evolution of the magnetic field. It is the same in form as the propagation law for vorticity  $\boldsymbol{\omega}$  in a flow with  $\nabla P \times \nabla \rho = 0$  [Eq. (14.3), or (14.6) with  $\boldsymbol{\omega} \nabla \cdot \mathbf{v}$  added in the compressible case]. The  $\nabla \times (\mathbf{v} \times \mathbf{B})$  term in Eq. (19.6) dominates when the conductivity is large and can be regarded as describing the freezing of magnetic field lines in the fluid in the same way as the  $\nabla \times (\mathbf{v} \times \boldsymbol{\omega})$  term describes the freezing of vortex lines in a fluid with small viscosity  $\nu$  (Fig. 19.2). By analogy with Eq. (14.10), when flux-freezing dominates, the fluid derivative of  $\mathbf{B}/\rho$  can be written as

for large conductivity: freezing of magnetic field into the fluid

$$\frac{D}{Dt} \left( \frac{\mathbf{B}}{\rho} \right) \equiv \frac{d}{dt} \left( \frac{\mathbf{B}}{\rho} \right) - \left( \frac{\mathbf{B}}{\rho} \cdot \nabla \right) \mathbf{v} = 0, \quad (19.8)$$

where  $\rho$  is mass density (not to be confused with charge density  $\rho_e$ ). Equation (19.8) states that  $\mathbf{B}/\rho$  evolves in the same manner as the separation  $\Delta \mathbf{x}$  between two points in the fluid (cf. Fig. 14.4 and associated discussion).

The term  $[1/(\mu_0 \kappa_e)] \nabla^2 \mathbf{B}$  in the B-field evolution equation (19.6) or (19.7) is analogous to the vorticity diffusion term  $\nu \nabla^2 \boldsymbol{\omega}$  in the vorticity evolution equation (14.3) or (14.6). Therefore, when  $\kappa_e$  is not too large, magnetic field lines will diffuse through the fluid. The effective diffusion coefficient (analogous to  $\nu$ ) is

magnetic diffusion coefficient

$$D_M = 1/(\mu_0 \kappa_e). \quad (19.9a)$$

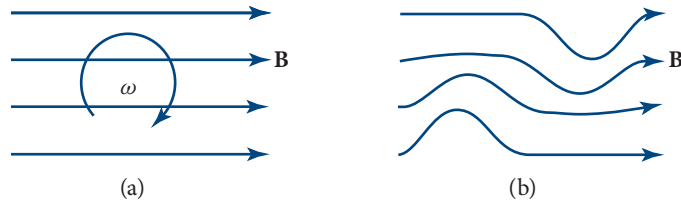


**FIGURE 19.2** Pictorial representation of the evolution of the magnetic field in a fluid endowed with infinite electrical conductivity. (a) A uniform magnetic field at time  $t = 0$  in a vortex. (b) At a later time, when the fluid has rotated through  $\sim 30^\circ$ , the circulation has stretched and distorted the magnetic field.

Earth's magnetic field provides an example of field diffusion. That field is believed to be supported by electric currents flowing in Earth's iron core. Now, we can estimate the electric conductivity of iron under these conditions and from it deduce a value for the diffusivity,  $D_M \sim 1 \text{ m}^2 \text{ s}^{-1}$ . The size of Earth's core is  $L \sim 10^4 \text{ km}$ , so if there were no fluid motions, then we would expect the magnetic field to diffuse out of the core and escape from Earth in a time

$$\tau_M \sim \frac{L^2}{D_M} \quad (19.9b)$$

magnetic decay time

$\sim 3$  million years, which is much shorter than the age of Earth,  $\sim 5$  billion years. The reason for this discrepancy, as we discuss in Sec. 19.6, is that there are internal circulatory motions in the liquid core that are capable of regenerating the magnetic field through dynamo action.

Although Eq. (19.6) describes a genuine diffusion of the magnetic field, to compute with confidence the resulting magnetic decay time, one must solve the complete boundary value problem. To give a simple illustration, suppose that a poor conductor (e.g., a weakly ionized column of plasma) is surrounded by an excellent conductor (e.g., the metal walls of the container in which the plasma is contained), and that magnetic field lines supported by wall currents thread the plasma. The magnetic field will only diminish after the wall currents undergo Ohmic dissipation, which can take much longer than the diffusion time for the plasma column alone.

It is customary to introduce a dimensionless number called the *magnetic Reynolds number*,  $R_M$ , directly analogous to the fluid Reynolds number  $Re$ , to describe the relative importance of flux freezing and diffusion. The fluid Reynolds number can be regarded as the ratio of the magnitude of the vorticity-freezing term,  $\nabla \times (\mathbf{v} \times \boldsymbol{\omega}) \sim (V/L)\boldsymbol{\omega}$ , in the vorticity evolution equation,  $\partial \boldsymbol{\omega} / \partial t = \nabla \times (\mathbf{v} \times \boldsymbol{\omega}) + \nu \nabla^2 \boldsymbol{\omega}$ , to the magnitude of the diffusion term,  $\nu \nabla^2 \boldsymbol{\omega} \sim (\nu/L^2)\boldsymbol{\omega}$ :  $Re = (V/L)(\nu/L^2)^{-1} = VL/\nu$ . Here  $V$  is a characteristic speed, and  $L$  a characteristic lengthscale of the flow. Similarly, the magnetic Reynolds number is the ratio of the magnitude of the

**TABLE 19.1:** Characteristic magnetic diffusivities  $D_M$ , decay times  $\tau_M$ , and magnetic Reynolds numbers  $R_M$  for some common MHD flows with characteristic length scales  $L$  and velocities  $V$

Substance	$L$ (m)	$V$ (m s <sup>-1</sup> )	$D_M$ (m <sup>2</sup> s <sup>-1</sup> )	$\tau_M$ (s)	$R_M$
Mercury	0.1	0.1	1	0.01	0.01
Liquid sodium	0.1	0.1	0.1	0.1	0.1
Laboratory plasma	1	100	10	0.1	10
Earth's core	10 <sup>7</sup>	0.1	1	10 <sup>14</sup>	10 <sup>6</sup>
Interstellar gas	10 <sup>17</sup>	10 <sup>3</sup>	10 <sup>3</sup>	10 <sup>31</sup>	10 <sup>17</sup>

magnetic-flux-freezing term,  $\nabla \times (\mathbf{v} \times \mathbf{B}) \sim (V/L)B$ , to the magnitude of the magnetic-flux-diffusion term,  $D_M \nabla^2 \mathbf{B} = [1/(\mu_0 \kappa_e)] \nabla^2 \mathbf{B} \sim B/(\mu_0 \kappa_e L^2)$ , in the induction equation (19.6):

$$R_M = \frac{V/L}{D_M/L^2} = \frac{VL}{D_M} = \mu_0 \kappa_e VL. \quad (19.9c)$$

When  $R_M \gg 1$ , the field lines are effectively frozen in the fluid; when  $R_M \ll 1$ , Ohmic dissipation is dominant, and the field lines easily diffuse through the fluid.

Magnetic Reynolds numbers and diffusion times for some typical MHD flows are given in Table 19.1. For most laboratory conditions,  $R_M$  is modest, which means that electric resistivity  $1/\kappa_e$  is significant, and the magnetic diffusivity  $D_M$  is rarely negligible. By contrast, in space physics and astrophysics,  $R_M$  is usually very large,  $R_M \gg 1$ , so the resistivity can be ignored almost always and everywhere. This limiting case, when the electric conductivity is treated as infinite, is often called *perfect MHD*.

The phrase “almost always and everywhere” needs clarification. Just as for large-Reynolds-number fluid flows, so also here, boundary layers and discontinuities can be formed, in which the gradients of physical quantities are automatically large enough to make  $R_M \sim 1$  locally. An important example discussed in Sec. 19.6.3 is *magnetic reconnection*. This occurs when regions magnetized along different directions are juxtaposed, for example, when the solar wind encounters Earth's magnetosphere. In such discontinuities and boundary layers, the current density is high, and magnetic diffusion and Ohmic dissipation are important. As in ordinary fluid mechanics, these dissipative layers and discontinuities can control the character of the overall flow despite occupying a negligible fraction of the total volume.

## 19.2.2 Momentum and Energy Conservation

The fluid dynamical aspects of MHD are handled by adding an electromagnetic force term to the Euler or Navier-Stokes equation. The magnetic force density  $\mathbf{j} \times \mathbf{B}$  is the sum of the Lorentz forces acting on all the fluid's charged particles in a unit volume.

magnetic Reynolds number and magnetic field freezing

perfect MHD: infinite conductivity and magnetic field freezing

magnetic reconnection and its influence

There is also an electric force density  $\rho_e \mathbf{E}$ , but this is smaller than  $\mathbf{j} \times \mathbf{B}$  by a factor  $O(v^2/c^2)$  by virtue of Eqs. (19.5), so we ignore it. When  $\mathbf{j} \times \mathbf{B}$  is added to the Euler equation (13.44) (or equivalently, to the Navier-Stokes equation with the viscosity neglected as unimportant in the situations we shall study), it takes the following form:

$$\rho \frac{d\mathbf{v}}{dt} = \rho \mathbf{g} - \nabla P + \mathbf{j} \times \mathbf{B} = \rho \mathbf{g} - \nabla P + \frac{(\nabla \times \mathbf{B}) \times \mathbf{B}}{\mu_0}. \quad (19.10)$$

MHD equation of motion for fluid

Here, we have used expression (19.5a) for the current density in terms of the magnetic field. This is our basic MHD force equation. In Sec. 20.6.2 we will generalize it to situations where, due to electron cyclotron motion, the pressure  $P$  is anisotropic.

Like all other force densities in this equation, the magnetic one  $\mathbf{j} \times \mathbf{B}$  can be expressed as minus the divergence of a stress tensor, the magnetic portion of the Maxwell stress tensor:

$$\mathbf{T}_M = \frac{B^2 \mathbf{g}}{2\mu_0} - \frac{\mathbf{B} \otimes \mathbf{B}}{\mu_0}; \quad (19.11)$$

magnetic stress tensor

see Ex. 19.1. By virtue of  $\mathbf{j} \times \mathbf{B} = -\nabla \cdot \mathbf{T}_M$  and other relations explored in Sec. 13.5 and Box 13.4, we can convert the force-balance equation (19.10) into the conservation law for momentum [generalization of Eq. (13.42)]:

momentum conservation

$$\frac{\partial(\rho \mathbf{v})}{\partial t} + \nabla \cdot (P \mathbf{g} + \rho \mathbf{v} \otimes \mathbf{v} + \mathbf{T}_g + \mathbf{T}_M) = 0. \quad (19.12)$$

Here  $\mathbf{T}_g$  is the gravitational stress tensor [Eq. (1) of Box 13.4], which resembles the magnetic one:

$$\mathbf{T}_g = -\frac{g^2 \mathbf{g}}{8\pi G} + \frac{\mathbf{g} \otimes \mathbf{g}}{4\pi G}; \quad (19.13)$$

it is generally unimportant in laboratory plasmas but can be quite important in and near stars and black holes.

The two terms in the magnetic Maxwell stress tensor [Eq. (19.11)] can be identified as the “push” of an isotropic magnetic pressure of  $B^2/(2\mu_0)$  that acts just like the gas pressure  $P$ , and the “pull” of a tension  $B^2/\mu_0$  that acts parallel to the magnetic field. The combination of the tension and the isotropic pressure give a net tension  $B^2/(2\mu_0)$  along the field and a net pressure  $B^2/(2\mu_0)$  perpendicular to the field lines (Ex. 1.14).

The magnetic force density

magnetic force density

$$\mathbf{f}_m = -\nabla \cdot \mathbf{T}_M = \mathbf{j} \times \mathbf{B} = \frac{(\nabla \times \mathbf{B}) \times \mathbf{B}}{\mu_0} \quad (19.14)$$

can be rewritten, using standard vector identities, as

$$\mathbf{f}_m = -\nabla \left( \frac{B^2}{2\mu_0} \right) + \frac{(\mathbf{B} \cdot \nabla) \mathbf{B}}{\mu_0} = - \left[ \nabla \left( \frac{B^2}{2\mu_0} \right) \right]_{\perp} + \left[ \frac{(\mathbf{B} \cdot \nabla) \mathbf{B}}{\mu_0} \right]_{\perp}. \quad (19.15)$$

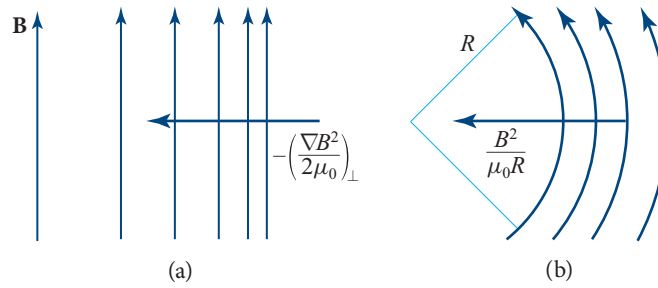


**FIGURE 19.3** Contributions to the electromagnetic force density acting on a conducting fluid in a nonuniform magnetic field. A magnetic-pressure force density  $-\left[\nabla B^2/(2\mu_0)\right]_\perp$  acts perpendicularly to the field. And a magnetic-curvature force density  $[(\mathbf{B} \cdot \nabla)\mathbf{B}/\mu_0]_\perp$ , which is also perpendicular to the magnetic field and lies in the plane of the field’s bend, points toward its center of curvature. The magnitude of this curvature force density is  $B^2/(\mu_0 R)$ , where  $R$  is the radius of curvature.

Here “ $\perp$ ” means keep only the components perpendicular to the magnetic field; the fact that  $\mathbf{f}_m = \mathbf{j} \times \mathbf{B}$  guarantees that the net force parallel to  $\mathbf{B}$  must vanish, so we can throw away the component along  $\mathbf{B}$  in each term. This transversality of  $\mathbf{f}_m$  means that the magnetic force neither inhibits nor promotes motion of the fluid along the magnetic field. Instead, fluid elements are free to slide along the field like beads that slide without friction along a magnetic “wire.”

The “ $\perp$ ” expressions in Eq. (19.15) indicate that the magnetic force density has two parts: first, the negative of the 2-dimensional gradient of the magnetic pressure  $B^2/(2\mu_0)$  orthogonal to  $\mathbf{B}$  (Fig. 19.3a), and second, an orthogonal *curvature force*  $(\mathbf{B} \cdot \nabla)\mathbf{B}/\mu_0$ , which has magnitude  $B^2/(\mu_0 R)$ , where  $R$  is the radius of curvature of a field line. This curvature force acts toward the field line’s center of curvature (Fig. 19.3b) and is the magnetic-field-line analog of the force that acts on a curved wire or curved string under tension.

Just as the magnetic force density dominates and the electric force is negligible  $[O(v^2/c^2)]$  in our nonrelativistic situation, so also the electromagnetic contribution to the energy density is predominantly due to the magnetic term  $U_M = B^2/(2\mu_0)$  with negligible electric contribution. The electromagnetic energy flux is just the Poynting flux  $\mathbf{F}_M = \mathbf{E} \times \mathbf{B}/\mu_0$ , with  $\mathbf{E}$  given by Eq. (19.5b). Inserting these expressions into the law of energy conservation (13.58) (and continuing to neglect viscosity), we obtain

energy conservation

$$\frac{\partial}{\partial t} \left[ \left( \frac{1}{2}v^2 + u + \Phi \right) \rho + \frac{B^2}{2\mu_0} \right] + \nabla \cdot \left[ \left( \frac{1}{2}v^2 + h + \Phi \right) \rho \mathbf{v} + \frac{\mathbf{E} \times \mathbf{B}}{\mu_0} \right] = 0. \quad (19.16)$$

When the fluid’s self-gravity is important, we must augment this equation with the gravitational energy density and flux, as discussed in Box 13.4.

As in Sec. 13.7.4, we can combine this energy conservation law with mass conservation and the first law of thermodynamics to obtain an equation for the evolution of entropy: Eqs. (13.75) and (13.76) are modified to read

$$\frac{\partial(\rho s)}{\partial t} + \nabla \cdot (\rho s \mathbf{v}) = \rho \frac{ds}{dt} = \frac{j^2}{\kappa_e T}. \quad (19.17)$$

entropy evolution; Ohmic dissipation

Thus, just as viscosity increases entropy through viscous dissipation, and thermal conductivity increases entropy through diffusive heat flow [Eqs. (13.75) and (13.76)], so also electrical resistivity (formally,  $\kappa_e^{-1}$ ) increases entropy through Ohmic dissipation. From Eq. (19.17) we see that our fourth transport coefficient  $\kappa_e$ , like our previous three (the two coefficients of viscosity  $\eta \equiv \rho \nu$  and  $\zeta$  and the thermal conductivity  $\kappa$ ), is constrained to be positive by the second law of thermodynamics.

### Exercise 19.1 Derivation: Basic Equations of MHD

### EXERCISES

- Verify that  $-\nabla \cdot \mathbf{T}_M = \mathbf{j} \times \mathbf{B}$ , where  $\mathbf{T}_M$  is the magnetic stress tensor (19.11).
- Take the scalar product of the fluid velocity  $\mathbf{v}$  with the equation of motion (19.10) and combine with mass conservation to obtain the energy conservation equation (19.16).
- Combine energy conservation (19.16) with the first law of thermodynamics and mass conservation to obtain Eq. (19.17) for the evolution of the entropy.

### 19.2.3 Boundary Conditions

### 19.2.3

The equations of MHD must be supplemented by boundary conditions at two different types of interfaces. The first is a *contact discontinuity* (i.e., the interface between two distinct media that do not mix; e.g., the surface of a liquid metal or a rigid wall of a plasma containment device). The second is a shock front that is being crossed by the fluid. Here the boundary is between shocked and unshocked fluid.

types of interfaces: contact discontinuity and shock front

We can derive the boundary conditions by transforming into a primed frame in which the interface is instantaneously at rest (not to be confused with the fluid's local rest frame) and then transforming back into our original unprimed inertial frame. In the primed frame, we resolve the velocity and magnetic and electric vectors into components normal and tangential to the surface. If  $\mathbf{n}$  is a unit vector normal to the surface, then the normal and tangential components of velocity in either frame are

$$v_n = \mathbf{n} \cdot \mathbf{v}, \quad \mathbf{v}_t = \mathbf{v} - (\mathbf{n} \cdot \mathbf{v})\mathbf{n}, \quad (19.18)$$

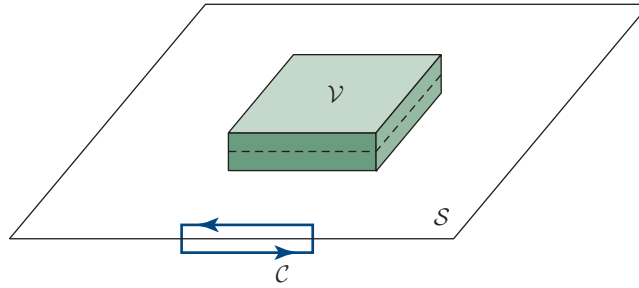


FIGURE 19.4 Elementary pill box  $\mathcal{V}$  and elementary circuit  $\mathcal{C}$  used in deriving the MHD junction conditions at a surface  $\mathcal{S}$ .

and similarly for the  $\mathbf{E}$  and  $\mathbf{B}$ . At a contact discontinuity, we have

$$v'_n = v_n - v_{sn} = 0 \quad (19.19a)$$

on both sides of the interface surface; here  $v_{sn}$  is the normal velocity of the surface. At a shock front, mass flux across the surface is conserved [cf. Eq. (17.29a)]:

$$[\rho v'_n] = [\rho(v_n - v_{sn})] = 0. \quad (19.19b)$$

Here, as in Sec. 17.5, we use the notation  $[X]$  to signify the difference in some quantity  $X$  across the interface, that is, the *junction condition* for  $X$ .

When we consider the magnetic field, it does not matter which frame we use, since  $\mathbf{B}$  is unchanged to the Galilean order at which we are working. Let us construct a thin “pill box”  $\mathcal{V}$  (Fig. 19.4) and integrate the equation  $\nabla \cdot \mathbf{B} = 0$  over its volume, invoke the divergence theorem, and let the box thickness diminish to zero; thereby we see that

$$[B_n] = 0. \quad (19.19c)$$

By contrast, the tangential component of the magnetic field can be discontinuous across an interface because of surface currents: by integrating  $\nabla \times \mathbf{B} = \mu_0 \mathbf{j}$  across the shock front, we can deduce that

$$[\mathbf{B}_t] = -\mu_0 \mathbf{n} \times \mathbf{J}, \quad (19.19d)$$

where  $\mathbf{J}$  is the surface current density.

We deduce the junction condition on the electric field by integrating Maxwell’s equation  $\nabla \times \mathbf{E} = -\partial \mathbf{B} / \partial t$  over the area bounded by the circuit  $\mathcal{C}$  in Fig. 19.4 and using Stokes’ theorem, letting the two short legs of the circuit vanish. We thereby obtain

$$[\mathbf{E}'_t] = [\mathbf{E}_t] + [(\mathbf{v}_s \times \mathbf{B})_t] = 0, \quad (19.19e)$$

boundary conditions at interfaces: Eqs. (19.19)

junction condition for mass flux

electromagnetic junction conditions

where  $\mathbf{v}_s$  is the velocity of a frame that moves with the surface. Note that only the normal component of the velocity contributes to this expression, so we can replace  $\mathbf{v}_s$  by  $v_{sn}\mathbf{n}$ . The normal component of the electric field, like the tangential component of the magnetic field, can be discontinuous, as there may be surface charge at the interface.

There are also dynamical junction conditions that can be deduced by integrating the laws of momentum conservation (19.12) and energy conservation (19.16) over the pill box and using Gauss's theorem to convert the volume integral of a divergence to a surface integral. The results, naturally, are the requirements that the normal fluxes of momentum  $\mathbf{T} \cdot \mathbf{n}$  and energy  $\mathbf{F} \cdot \mathbf{n}$  be continuous across the surface. Here  $\mathbf{T}$  is the total stress [i.e., the quantity inside the divergence in Eq. (19.12)], and  $\mathbf{F}$  is the total energy flux [i.e., the quantity inside the divergence in Eq. (19.16)]; see Eqs. (17.29)–(17.31) and associated discussion. The normal and tangential components of  $[\mathbf{T} \cdot \mathbf{n}] = 0$  read

$$\left[ P + \rho(v_n - v_{sn})^2 + \frac{B_t^2}{2\mu_0} \right] = 0, \quad (19.19f)$$

dynamical junction conditions

$$\left[ \rho(v_n - v_{sn})(\mathbf{v}_t - \mathbf{v}_{st}) - \frac{B_n \mathbf{B}_t}{\mu_0} \right] = 0, \quad (19.19g)$$

where we have omitted the gravitational stress, since it will always be continuous in situations studied in this chapter (no surface layers of mass). Similarly, continuity of the energy flux  $[\mathbf{F} \cdot \mathbf{n}] = 0$  reads

$$\left[ \left( \frac{1}{2}v^2 + h \right) \rho(v_n - v_{sn}) + \frac{\mathbf{n} \cdot [(\mathbf{E} + \mathbf{v}_s \times \mathbf{B}) \times \mathbf{B}]}{\mu_0} \right] = 0. \quad (19.19h)$$

When the interface has plasma on one side and a vacuum magnetic field on the other, as in devices for magnetic confinement of plasmas (Sec. 19.3), the vacuum electromagnetic field, like that in the plasma, has small time derivatives:  $\partial/\partial t \sim v\partial/\partial x^j$ . As a result, the vacuum displacement current  $\epsilon_0\partial\mathbf{E}/\partial t$  is very small, and the vacuum Maxwell equations reduce to the same form as those in the MHD plasma but with  $\rho_e$  and  $\mathbf{j}$  zero. As a result, the boundary conditions at the vacuum-plasma interface (Ex. 19.2) are those discussed above [Eqs. (19.19)], but with  $\rho$  and  $P$  vanishing on the vacuum side.

### Exercise 19.2 *Example and Derivation: Perfect MHD Boundary Conditions at a Fluid-Vacuum Interface*

## EXERCISES

When analyzing the stability of configurations for magnetic confinement of a plasma (Sec. 19.5), one needs boundary conditions at the plasma-vacuum interface for the special case of perfect MHD (electrical conductivity idealized as arbitrarily large).

Denote by a tilde ( $\tilde{\mathbf{B}}$  and  $\tilde{\mathbf{E}}$ ) the magnetic and electric fields in the vacuum, and reserve non-tilde symbols for quantities on the plasma side of the interface.

- (a) Show that the normal-force boundary condition (19.19f) reduces to an equation for the vacuum region's tangential magnetic field:

$$\frac{\tilde{B}_t^2}{2\mu_0} = P + \frac{B_t^2}{2\mu_0}. \quad (19.20a)$$

- (b) By combining Eqs. (19.19c) and (19.19g) and noting that  $v_n - v_{sn}$  must vanish (why?), and assuming that the magnetic confinement entails surface currents on the interface, show that the normal component of the magnetic field must vanish on both sides of the interface:

$$\tilde{B}_n = B_n = 0. \quad (19.20b)$$

- (c) When analyzing energy flow across the interface, it is necessary to know the tangential electric field. On the plasma side  $\tilde{\mathbf{E}}_t$  is a secondary quantity fixed by projecting tangentially the relation  $\mathbf{E} + \mathbf{v} \times \mathbf{B} = 0$ . On the vacuum side it is fixed by the boundary condition (19.19e). By combining these two relations, show that

$$\tilde{\mathbf{E}}_t + \mathbf{v}_{sn} \times \tilde{\mathbf{B}}_t = 0. \quad (19.20c)$$

**Exercise 19.3** *Problem: Diffusion of Magnetic Field*

Consider an infinitely long cylinder of plasma with constant electric conductivity, surrounded by vacuum. Assume that the cylinder initially is magnetized uniformly parallel to its length, and assume that the field decays quickly enough that the plasma's inertia keeps it from moving much during the decay (so  $\mathbf{v} \simeq 0$ ).

- (a) Show that the reduction of magnetic energy as the field decays is compensated by the Ohmic heating of the plasma plus energy lost to outgoing electromagnetic waves (which will be negligible if the decay is slow).
- (b) Compute the approximate magnetic profile after the field has decayed to a small fraction of its original value. Your answer should be expressible in terms of a Bessel function.

**Exercise 19.4** *Example: Shock with Transverse Magnetic Field*

Consider a normal shock wave ( $\mathbf{v}$  perpendicular to the shock front), in which the magnetic field is parallel to the shock front, analyzed in the shock front's rest frame.

- (a) Show that the junction conditions across the shock are the vanishing of all the following quantities:

$$[\rho v] = [P + \rho v^2 + B^2/(2\mu_0)] = [h + v^2/2 + B^2/(\mu_0\rho)] = [vB] = 0. \quad (19.21)$$

- (b) Specialize to a fluid with equation of state  $P \propto \rho^\gamma$ . Show that these junction conditions predict no compression,  $[\rho] = 0$ , if the upstream velocity is  $v_1 = C_f \equiv \sqrt{(B_1^2/\mu_0 + \gamma P_1)/\rho_1}$ . For  $v_1$  greater than this  $C_f$ , the fluid gets compressed.

- (c) Explain why the result in part (b) means that the speed of sound perpendicular to the magnetic field must be  $C_f$ . As we shall see in Sec. 19.7.2, this indeed is the case:  $C_f$  is the speed [Eq. (19.77)] of a *fast magnetosonic wave*, the only kind of sound wave that can propagate perpendicular to  $\mathbf{B}$ .

**Exercise 19.5** *Problem: Earth's Bow Shock*

The solar wind is a supersonic, hydromagnetic flow of plasma originating in the solar corona. At the radius of Earth's orbit, the wind's density is  $\rho \sim 6 \times 10^{-21} \text{ kg m}^{-3}$ , its velocity is  $v \sim 400 \text{ km s}^{-1}$ , its temperature is  $T \sim 10^5 \text{ K}$ , and its magnetic field strength is  $B \sim 1 \text{ nT}$ .

- (a) By balancing the wind's momentum flux with the magnetic pressure exerted by Earth's dipole magnetic field, estimate the radius above Earth at which the solar wind passes through a bow shock (Fig. 17.2).
- (b) Consider a strong perpendicular shock at which the magnetic field is parallel to the shock front. Show that the magnetic field strength will increase by the same ratio as the density, when crossing the shock front. Do you expect the compression to increase or decrease as the strength of the field is increased, keeping all of the other flow variables constant?

19.2.4 Magnetic Field and Vorticity

19.2.4

We have already remarked on how the magnetic field and the vorticity are both axial vectors that can be written as the curl of a polar vector and that they satisfy similar transport equations. It is not surprising that they are physically intimately related. To explore this relationship in full detail would take us beyond the scope of this book. However, we can illustrate their interaction by showing how they can create each other. In brief: vorticity can twist a magnetic field, amplifying it; and an already twisted field, trying to untwist itself, can create vorticity.

vorticity-magnetic-field interactions

First, consider a simple vortex through which passes a uniform magnetic field (Fig. 19.2a). If the magnetic Reynolds number is large enough, then the magnetic field is carried with the flow and is wound up like spaghetti on the end of a fork (Fig. 19.2b, continued for a longer time). This process increases the magnetic energy in the vortex, though not the mean flux of the magnetic field. This amplification continues until either the field gradient is large enough that the field decays through Ohmic dissipation, or the field strength is large enough to react back on the flow and stop it from spinning.

Second, consider an irrotational flow containing a twisted magnetic field (Fig. 19.5a). Provided that the magnetic Reynolds number is sufficiently large, the magnetic stress, attempting to untwist the field, will act on the flow and induce vorticity (Fig. 19.5b). We can describe this formally by taking the curl of the equation

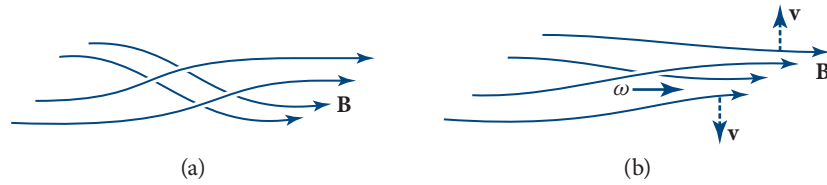


**FIGURE 19.5** (a) A twisted magnetic field is frozen in an irrotational flow. (b) The field tries to untwist and in the process creates vorticity.

of motion (19.10). Assuming, for simplicity, that the density  $\rho$  is constant and the electric conductivity is infinite, we obtain

$$\frac{\partial \boldsymbol{\omega}}{\partial t} - \nabla \times (\mathbf{v} \times \boldsymbol{\omega}) = \frac{\nabla \times [(\nabla \times \mathbf{B}) \times \mathbf{B}]}{\mu_0 \rho}. \quad (19.22)$$

The term on the right-hand side of this equation changes the number of vortex lines threading the fluid, just like the  $-\nabla P \times \nabla \rho / \rho^2$  term on the right-hand side of Eq. (14.3). However, because the divergence of the vorticity is zero, any fresh vortex lines that are made must be created as continuous curves that grow out of points or lines where the vorticity vanishes.

## 19.3

### 19.3 Magnetostatic Equilibria

#### 19.3.1

#### 19.3.1 Controlled Thermonuclear Fusion

##### GLOBAL POWER DEMAND

We start this section with an oversimplified discussion of the underlying problem. Earth's population has quadrupled over the past century to its present (2016) value of 7.4 billion and is still rising. We consume  $\sim 16$  TW of power more or less equally for manufacture, transportation, and domestic use. The power is derived from oil ( $\sim 5$  TW), coal ( $\sim 4$  TW), gas ( $\sim 4$  TW), nuclear (fission) reactors ( $\sim 1$  TW), hydroelectric turbines ( $\sim 1$  TW), and alternative sources, such as solar, wind, wave, and biomass ( $\sim 1$  TW). The average power consumption is  $\sim 2$  kW per person, with Canada and the United States in the lead, consuming  $\sim 10$  kW per person. Despite conservation efforts, the demand for energy still appears to be rising.

Meanwhile, the burning of coal, oil, and gas produces carbon dioxide at a rate of  $\sim 1 \text{ Gg s}^{-1}$ , about 10% of the total transfer rate in Earth's biomass–atmosphere–ocean *carbon cycle*. This disturbance of the carbon-cycle equilibrium has led to an increase in the atmospheric concentration of carbon dioxide by about a third over the past century and it is currently growing at an average rate of about a half percent per year. There is strong evidence to link this increase in carbon dioxide and other greenhouse gases to climate change, as exemplified by an increase in the globally averaged mean temperature of  $\sim 1$  K over the past century. Given the long time constants associated with the three components of the carbon cycle, future projections of climate change

motivation for controlled fusion program

are alarming. These considerations strongly motivate the rapid deployment of low-carbon sources of power—renewables and nuclear—and conservation.

#### THERMONUCLEAR FUSION

For more than 60 years, plasma physicists have striven to address this problem by releasing nuclear energy in a controlled, peaceful manner through confining plasma at a temperature in excess of 100 million degrees using strong magnetic fields. In the most widely studied scheme, deuterium and tritium combine according to the reaction



d, t fusion reaction

The energy release is equivalent to  $\sim 400 \text{ TJ kg}^{-1}$ . The fast neutrons can be absorbed in a surrounding blanket of lithium, and the heat can then be used to drive a generator.

#### PLASMA CONFINEMENT

At first this task seemed quite simple. However, it eventually became clear that it is very difficult to confine hot plasma with a magnetic field, because most confinement geometries are unstable. In this book we restrict our attention to a few simple confinement devices, emphasizing the one that is the basis of most modern efforts, the *tokamak*.<sup>1</sup> In this section, we treat equilibrium configurations; in Sec. 19.5, we consider their stability.

In our discussions of both equilibrium and stability, we treat the plasma as a magnetized fluid in the MHD approximation. At first sight, treating the plasma as a fluid might seem rather unrealistic, because we are dealing with a dilute gas of ions and electrons that undergo infrequent Coulomb collisions. However, as we discuss in Sec. 20.5.2 and justify in Chaps. 22 and 23, collective effects produce a sufficiently high effective collision frequency to make the plasma behave like a fluid, so MHD is usually a good approximation for describing these equilibria and their rather slow temporal evolution.

Let us examine some numbers that characterize the regime in which a successful controlled-fusion device must operate.

#### PLASMA PRESSURE

The ratio of plasma pressure to magnetic pressure

$$\beta \equiv \frac{P}{B^2/(2\mu_0)} \quad (19.24)$$

pressure ratio  $\beta$  for controlled fusion

plays a key role. For the magnetic field to have any chance of confining the plasma, its pressure must exceed that of the plasma (i.e.,  $\beta$  must be less than one). The most successful designs achieve  $\beta \sim 0.2$ . The largest field strengths that can be safely

1. Originally proposed in the Soviet Union by Andrei Sakharov and Igor Tamm in 1950. The word is a Russian abbreviation for “toroidal magnetic field.”

maximum gas pressure for magnetic confinement

sustained in the laboratory are  $B \sim 10 \text{ T} = 100 \text{ kG}$ , so  $\beta \lesssim 0.2$  limits the gas pressure to  $P \lesssim 10^7 \text{ Pa} \sim 100 \text{ atmospheres}$ .

#### LAWSON CRITERION

Plasma fusion can only be economically feasible if more power is released by nuclear reactions than is lost to radiative cooling. Both heating and cooling are proportional to the square of the number density of hydrogen ions,  $n^2$ . However, while the radiative cooling rate increases comparatively slowly with temperature, the nuclear reaction rate increases very rapidly. (This is because, as the mean energy of the ions increases, the number of ions in the Maxwellian tail of the distribution function that are energetic enough to penetrate the Coulomb barrier increases exponentially.) Thus for the rate of heat production to greatly exceed the rate of cooling, the temperature need only be modestly higher than that required for the rates to be equal—which is a minimum temperature essentially fixed by atomic and nuclear physics. In the case of a d-t plasma, this is  $T_{\min} \sim 10^8 \text{ K}$ . The maximum hydrogen density that can be confined is therefore  $n_{\max} = P/(2k_B T_{\min}) \sim 3 \times 10^{21} \text{ m}^{-3}$ . (The factor 2 comes from the electrons, which produce the same pressure as the ions.)

minimum temperature for fusion and maximum density for confinement

Now, if a volume  $V$  of plasma is confined at a given number density  $n$  and temperature  $T_{\min}$  for a time  $\tau$ , then the amount of nuclear energy generated will be proportional to  $n^2 V \tau$ , while the energy to heat the plasma up to  $T_{\min}$  is  $\propto nV$ . Therefore, there is a minimum value of the product  $n\tau$  that must be attained before net energy is produced. This condition is known as the *Lawson criterion*. Numerically, the plasma must be confined for

Lawson criterion for net energy production in controlled fusion

$$\tau \sim (n/10^{20} \text{ m}^{-3})^{-1} \text{ s}, \quad (19.25)$$

typically  $\sim 30 \text{ ms}$ . The sound speed at these temperatures is  $\sim 1 \times 10^6 \text{ m s}^{-1}$ , and so an unconfined plasma would hit the few-meter-sized walls of the vessel in which it is held in a few  $\mu\text{s}$ . Therefore, the magnetic confinement must be effective for typically  $10^4$ – $10^5$  dynamical timescales (sound-crossing times). It is necessary that the plasma be confined and confined well if we want to build a viable fusion reactor.

### 19.3.2

#### 19.3.2 Z-Pinch

Z-pinch configuration for plasma confinement

Before discussing plasma confinement by tokamaks, we describe a simpler confinement geometry known as the *Z-pinch* and often called the Bennett pinch (Fig. 19.6a). In a Z-pinch, electric current is induced to flow along a cylinder of plasma. This current creates a toroidal magnetic field whose tension prevents the plasma from expanding radially, much like hoops on a barrel prevent it from exploding. Let us assume that the cylinder has a radius  $R$  and is surrounded by vacuum.

Now, in static equilibrium we must balance the plasma pressure gradient by a Lorentz force:

$$\nabla P = \mathbf{j} \times \mathbf{B}. \quad (19.26)$$

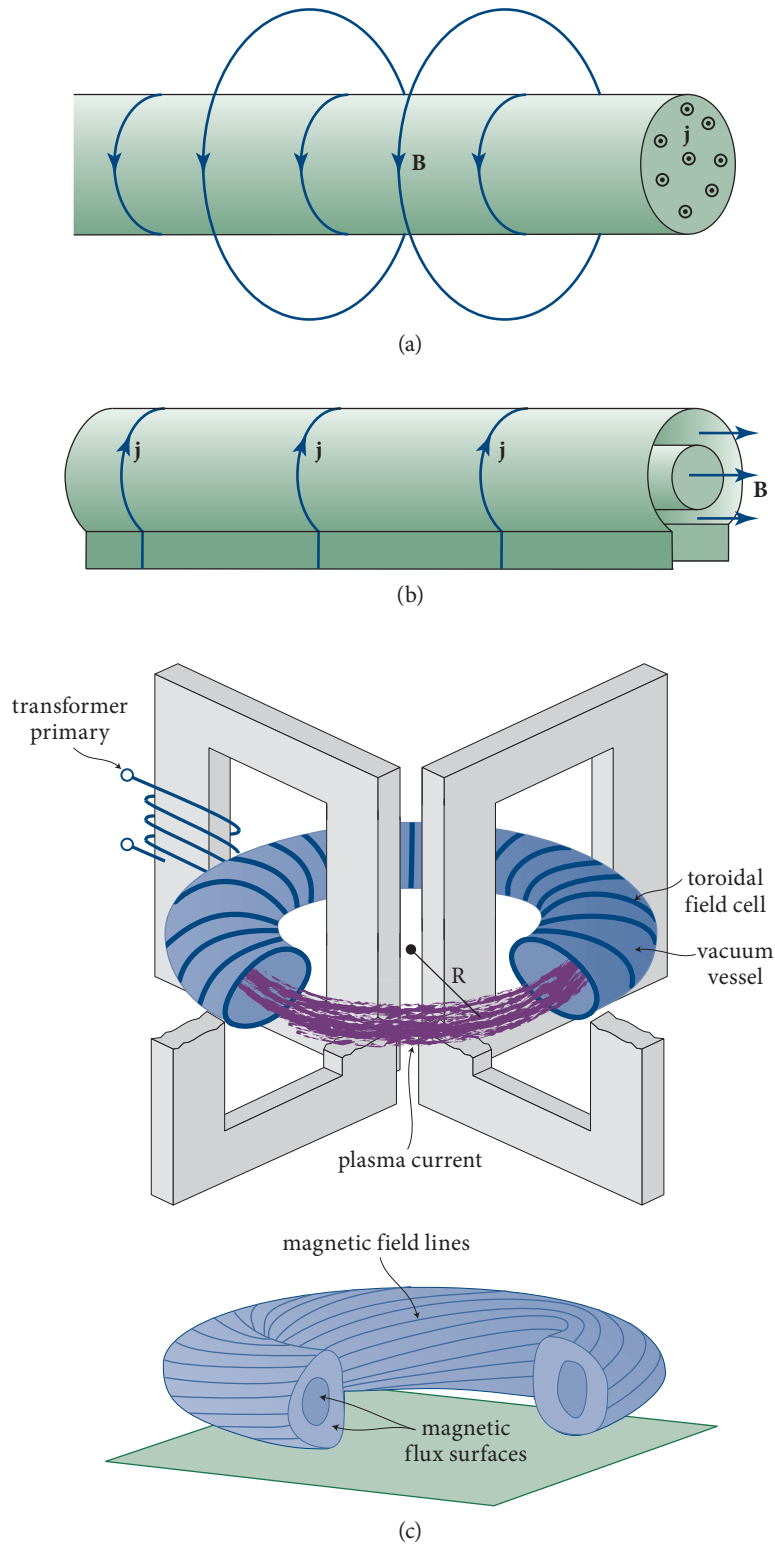


FIGURE 19.6 (a) The Z-pinch. (b) The  $\Theta$ -pinch. (c) The tokamak.

(Gravitational forces can safely be ignored.) Equation (19.26) implies immediately that  $\mathbf{B} \cdot \nabla P = \mathbf{j} \cdot \nabla P = 0$ , so both the magnetic field and the current density lie on constant pressure (or *isobaric*) surfaces. An equivalent version of the force-balance equation (19.26), obtained using Eq. (19.15) and Fig. 19.3, is

$$\frac{d}{d\varpi} \left( P + \frac{B^2}{2\mu_0} \right) = -\frac{B^2}{\mu_0\varpi}, \quad (19.27)$$

where  $\varpi$  is the radial cylindrical coordinate. Equation (19.27) exhibits the balance between the gradient of plasma and magnetic pressure on the left, and the magnetic tension (the “hoop force”) on the right. Treating it as a differential equation for  $B^2$  and integrating it, assuming that  $P$  falls to zero at the surface of the column, we obtain for the surface magnetic field

$$B^2(R) = \frac{4\mu_0}{R^2} \int_0^R P\varpi d\varpi. \quad (19.28)$$

We can reexpress the surface toroidal field in terms of the total current flowing along the plasma as  $B(R) = \mu_0 I / (2\pi R)$  (Ampère’s law); and assuming that the plasma is primarily hydrogen (so its ion density  $n$  and electron density are equal), we can write the pressure as  $P = 2nk_B T$ . Inserting these expressions into Eq. (19.28), integrating, and solving for the current, we obtain

$$I = \left( \frac{16\pi N k_B T}{\mu_0} \right)^{1/2}, \quad (19.29)$$

where  $N$  is the number of ions per unit length. For a column of plasma with diameter  $2R \sim 1$  m, hydrogen density  $n \sim 10^{20} \text{ m}^{-3}$ , and temperature  $T \sim 10^8$  K, Eq. (19.29) indicates that currents  $\sim 1$  MA are required for confinement.

The most promising Z-pinch experiments to date have been carried out at Sandia National Laboratories in Albuquerque, New Mexico. The experimenters have impulsively compressed a column of gas into a surprisingly stable cylinder of diameter  $\sim 1$  mm for a time  $\sim 100$  ns, using a current of  $\sim 30$  MA from giant capacitor banks. A transient field of  $\sim 1$  kT was created.

### 19.3.3

### 19.3.3 $\ominus$ -Pinch

**$\ominus$ -pinch configuration for plasma confinement**

There is a complementary equilibrium for a cylindrical plasma, in which the magnetic field lies parallel to the axis and the current density encircles the cylinder (Fig. 19.6b). This configuration is called the  $\ominus$ -pinch. It is usually established by making a cylindrical metal tube with a small gap, so that current can flow around it as shown in the figure. The tube is filled with cold plasma, and then the current is turned on quickly, producing a quickly growing longitudinal field in the tube (as in a solenoid). Since the plasma is highly conducting, the field lines cannot penetrate the plasma column but instead exert a pressure on its surface, causing it to shrink radially and rapidly. The plasma heats up due to both the radial work done on it and Ohmic heating. Equilibrium is established when the plasma’s pressure  $P$  balances the magnetic pressure  $B^2/(2\mu_0)$  at the plasma’s surface.

Despite early promise, interest in  $\Theta$ -pinches has waned, and mirror machines (Sec. 19.5.3) have become more popular.

#### 19.3.4 Tokamak

One of the problems with the  $\Theta$ - and Z-pinches (and we shall find other problems below!) is that they have ends through which plasma can escape. This is readily addressed by replacing the cylinder with a torus. The most stable geometry, called the *tokamak*, combines features of both Z- and  $\Theta$ -pinches; see Fig. 19.6c. If we introduce spherical coordinates  $(r, \theta, \phi)$ , then magnetic field lines and currents that lie in an  $r$ - $\theta$  plane (orthogonal to  $\mathbf{e}_\phi$ ) are called *poloidal*, whereas their  $\phi$  components are called *toroidal*. In a tokamak, the toroidal magnetic field is created by external poloidal current windings. However, the poloidal field is mostly created as a consequence of toroidal current induced to flow in the plasma torus. The resulting net field lines wrap around the plasma torus in a helical manner, defining a magnetic surface on which the pressure is constant. The number of poloidal transits around the torus during one toroidal transit is denoted  $\iota/(2\pi)$ ;  $\iota$  is called the *rotational transform* and is a property of the magnetic surface on which the field line resides. If  $\iota/(2\pi)$  is a rational number, then the field line will close after a finite number of circuits. However, in general,  $\iota/(2\pi)$  will not be rational, so a single field line will cover the whole magnetic surface ergodically. This allows the plasma to spread over the whole surface rapidly. The rotational transform is a measure of the toroidal current flowing inside the magnetic surface and of course increases as we move out from the innermost magnetic surface, while the pressure decreases.

The best performers to date (2016) include the MIT Alcator C-Mod ( $n \sim 2 \times 10^{20} \text{ m}^{-3}$ ,  $T \sim 35 \text{ MK}$ ,  $B \sim 6 \text{ T}$ ,  $\tau \sim 2 \text{ s}$ ), and the larger Joint European Torus or JET (Keilhacker and the JET team, 1998). JET generated 16 MW of nuclear power with  $\tau \sim 1 \text{ s}$  by burning d-t fuel, but its input power was  $\sim 25 \text{ MW}$  and so, despite being a major step forward, JET fell short of achieving “break even.”

The largest device, currently under construction, is the International Thermonuclear Experimental Reactor (ITER) (whose acronym means “journey” in Latin). ITER is a tokamak-based experimental fusion reactor being constructed in France by a large international consortium (see <http://www.iter.org/>). The outer diameter of the device is  $\sim 20 \text{ m}$ , and the maximum magnetic field produced by its superconducting magnets will be  $\sim 14 \text{ T}$ . Its goal is to use d-t fuel to convert an input power of  $\sim 50 \text{ MW}$  into an output power of  $\sim 500 \text{ MW}$ , sustained for  $\sim 3,000 \text{ s}$ .<sup>2</sup> However, many engineering, managerial, financial, and political challenges remain to be addressed before mass production of economically viable, durable, and safe fusion reactors can begin.

2. Note that it would require of order 10,000 facilities with ITER's projected peak power operating continuously to supply, say, one-third of the current global power demand.

#### 19.3.4

tokamak configuration for plasma confinement

JET

ITER

## EXERCISES

### Exercise 19.6 *Problem: Strength of Magnetic Field in a Magnetic Confinement Device*

The currents that are sources for strong magnetic fields have to be held in place by solid conductors. Estimate the limiting field that can be sustained using normal construction materials.

### Exercise 19.7 *Problem: Force-Free Equilibria*

In an equilibrium state of a very low- $\beta$  plasma, the plasma's pressure force density  $-\nabla P$  is ignorably small, and so the Lorentz force density  $\mathbf{j} \times \mathbf{B}$  must vanish [Eq. (19.10)]. Such a plasma is said to be "force-free." As a result, the current density is parallel to the magnetic field, so  $\nabla \times \mathbf{B} = \alpha \mathbf{B}$ . Show that  $\alpha$  must be constant along a field line, and that if the field lines eventually travel everywhere, then  $\alpha$  must be constant everywhere.

### Exercise 19.8 *Example and Challenge: Spheromak*

Another magnetic confinement device which brings out some important principles is the *spheromak*. Spheromaks can be made in the laboratory (Bellan, 2000) and have also been proposed as the basis of a fusion reactor.<sup>3</sup> It is simplest to consider a spheromak in the limit when the plasma pressure is ignorable (low  $\beta$ ) and the magnetic field distribution is force-free (Ex. 19.7). We just describe the simplest example of this regime.

- (a) As in the previous exercise, assume that  $\alpha$  is constant everywhere and, without loss of generality, set it equal to unity. Show that the magnetic field—and also the current density and vector potential, adopting the Coulomb gauge—satisfy the vector Helmholtz equation:  $\nabla^2 \mathbf{B} + \alpha^2 \mathbf{B} = 0$ .
- (b) Introduce a scalar  $\chi$  such that  $\mathbf{B} = \alpha \mathbf{r} \times \nabla \chi + \nabla \times (\mathbf{r} \times \nabla \chi)$ , with  $\mathbf{r}$  the radial vector pointing out of the spheromak's center, and show that  $\chi$  satisfies the scalar Helmholtz equation:  $\nabla^2 \chi + \alpha^2 \chi = 0$ .
- (c) The Helmholtz equation in part (b) separates in spherical coordinates  $(r, \theta, \phi)$ . Show that it has a nonsingular solution  $\chi = j_l(\alpha r) Y_{lm}(\theta, \phi)$ , where  $j_l(\alpha r)$  is a spherical Bessel function, and  $Y_{lm}(\theta, \phi)$  is a spherical harmonic. Evaluate this for the simplest example, the spheromak, with  $l = 2$  and  $m = 0$ .
- (d) Calculate expressions for the associated magnetic field in part (c) and either sketch or plot it.
- (e) Show that the magnetic field's radial component vanishes on the surface of a sphere of radius equal to the first zero of  $j_l$ . Hence explain why a spheromak may be confined in a conducting sphere or, alternatively, by a current-free field that is uniform at large distance.

3. Spheromak configurations of magnetic fields have even been associated with ball lightning!

**Exercise 19.9** *Problem: Magnetic Helicity*

- (a) A physical quantity that turns out to be useful in describing the evolution of magnetic fields in confinement devices is *magnetic helicity*. This is defined by  $H = \int dV \mathbf{A} \cdot \mathbf{B}$ , where  $\mathbf{A}$  is the vector potential, and the integral should be performed over all the space visited by the field lines to remove a dependence on the electromagnetic gauge. Compute the partial derivative of  $\mathbf{A}$  and  $\mathbf{B}$  with respect to time to show that  $H$  is conserved if  $\mathbf{E} \cdot \mathbf{B} = 0$ .
- (b) The helicity  $H$  primarily measures the topological linkage of the magnetic field lines. Therefore, it should not be a surprise that  $H$  turns out to be relatively well-preserved, even when the plasma is losing energy through resistivity and radiation. To discuss magnetic helicity properly would take us too far into the domain of classical electromagnetic theory, but some indication of its value follows from computing it for the case of two rings of magnetic field containing fluxes  $\Phi_1$  and  $\Phi_2$ . Start with the rings quite separate, and show that  $H = 0$ . Then allow the rings to be linked while not sharing any magnetic field lines. Show that now  $H = 2\Phi_1\Phi_2$  and that  $dH/dt = -2 \int dV \mathbf{E} \cdot \mathbf{B}$ .<sup>4</sup>

**19.4 Hydromagnetic Flows**

We now introduce fluid motions into our applications of magnetohydrodynamics. Specifically, we explore a simple class of *stationary hydromagnetic flows*: the flow of an electrically conducting fluid along a duct of constant cross section perpendicular to a uniform magnetic field  $B_0$  (see Fig. 19.7). This is sometimes known as *Hartmann flow*. The duct has two insulating walls (top and bottom, as shown in the figure), separated by a distance  $2a$  that is much smaller than the separation of short side walls, which are electrically conducting.

To relate Hartmann flow to magnetic-free Poiseuille flow (viscous, laminar flow between plates; Ex. 13.18), we reinstate the viscous force in the equation of motion. For simplicity we assume that the time-independent flow ( $\partial \mathbf{v} / \partial t = 0$ ) has traveled sufficiently far down the duct ( $x$  direction) to have reached a  $z$ -independent form, so  $\mathbf{v} \cdot \nabla \mathbf{v} = 0$  and  $\mathbf{v} = \mathbf{v}(y, z)$ . We also assume that gravitational forces are unimportant. Then the flow's equation of motion takes the form

$$\nabla P = \mathbf{j} \times \mathbf{B} + \eta \nabla^2 \mathbf{v}, \tag{19.30}$$

where  $\eta = \rho \nu$  is the coefficient of dynamical viscosity. The magnetic (Lorentz) force  $\mathbf{j} \times \mathbf{B}$  alters the balance between the Poiseuille flow's viscous force  $\eta \nabla^2 \mathbf{v}$  and the

4. For further discussion, see Bellan (2000).

**19.4**

Hartmann flow and its applications

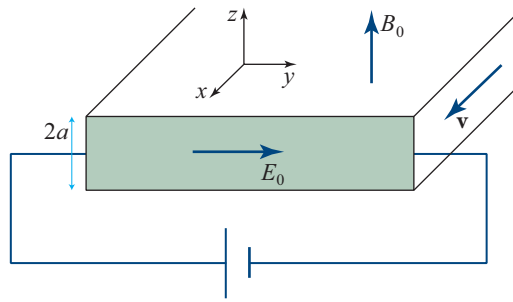


**FIGURE 19.7** Hartmann flow with average speed  $v$  along a duct of thickness  $2a$ , perpendicular to an applied magnetic field of strength  $B_0$ . The short side walls are conducting and the two long horizontal walls are electrically insulating.

four versions of Hartmann flow

pressure gradient  $\nabla P$ . The details of that altered balance and the resulting magnetic-influenced flow depend on how the walls are connected electrically. Let us consider four possibilities chosen to bring out the essential physics.

**ELECTROMAGNETIC BRAKE**

We short circuit the electrodes, so a current  $\mathbf{j}$  can flow (Fig. 19.8a). The magnetic field lines are partially dragged by the fluid, bending them (as embodied in  $\nabla \times \mathbf{B} = \mu_0 \mathbf{j}$ ), so they can exert a decelerating tension force  $\mathbf{j} \times \mathbf{B} = (\nabla \times \mathbf{B}) \times \mathbf{B} / \mu_0 = \mathbf{B} \cdot \nabla \mathbf{B} / \mu_0$  on the flow (Fig. 19.3b). This configuration is an electromagnetic brake. The pressure gradient, which is trying to accelerate the fluid, is balanced by the magnetic tension and viscosity. The work being done (per unit volume) by the pressure gradient,  $\mathbf{v} \cdot (-\nabla P)$ , is converted into heat through viscous and Ohmic dissipation.

**MHD POWER GENERATOR**

The MHD power generator is similar to the electromagnetic brake except that an external load is added to the circuit (Fig. 19.8b). Useful power can be extracted from the flow. Variants of this configuration were developed in the 1970s–1990s in many countries, but they are currently not seen to be economically competitive with other power-generation methods.

**FLOW METER**

When the electrodes in a flow meter are on an open circuit, the induced electric field produces a measurable potential difference across the duct (Fig. 19.8c). This voltage will increase monotonically with the rate of flow of fluid through the duct and therefore can provide a measurement of the flow.

**ELECTROMAGNETIC PUMP**

Finally, we can attach a battery to the electrodes and allow a current to flow (Figs. 19.7 and 19.8d). This produces a Lorentz force which either accelerates or decelerates the

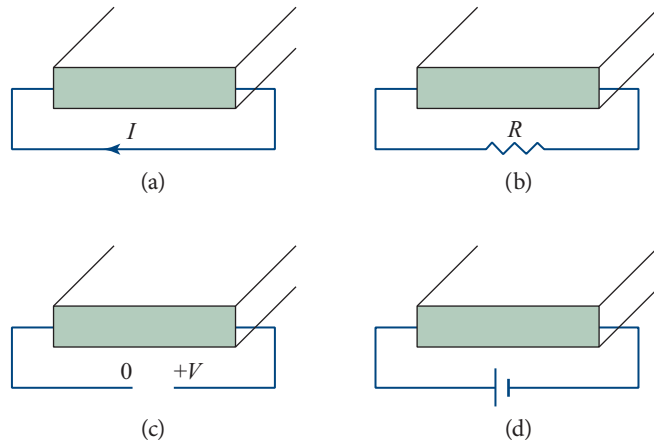


**FIGURE 19.8** Four variations on Hartmann flow: (a) Electromagnetic brake. (b) MHD power generator. (c) Flow meter. (d) Electromagnetic pump.

flow, depending on the direction of the magnetic field. This method can be used to pump liquid sodium coolant around a nuclear reactor. It has also been proposed as a means of spacecraft propulsion in interplanetary space.

We consider in more detail two limiting cases of the electromagnetic pump. When there is a constant pressure gradient  $Q = -dP/dx$  but no magnetic field, a flow with modest Reynolds number will be approximately laminar with velocity profile (Ex. 13.18):

$$v_x(z) = \frac{Qa^2}{2\eta} \left[ 1 - \left( \frac{z}{a} \right)^2 \right], \quad (19.31)$$

where  $a$  is the half-width of the channel. This flow is the 1-dimensional version of the Poiseuille flow in a pipe, such as a blood artery, which we studied in Sec. 13.7.6 [cf. Eq. (13.82a)]. Now suppose that uniform electric and magnetic fields  $E_0$  and  $B_0$  are applied along the  $\mathbf{e}_y$  and  $\mathbf{e}_z$  directions, respectively (Fig. 19.7). The resulting magnetic force  $\mathbf{j} \times \mathbf{B}$  can either reinforce or oppose the fluid's motion. When the applied magnetic field is small,  $B_0 \ll E_0/v_x$ , the effect of the magnetic force will be similar to that of the pressure gradient, and Eq. (19.31) must be modified by replacing  $Q \equiv -dP/dx$  by  $-dP/dx + j_y B_z = -dP/dy + \kappa_e E_0 B_0$ . [Here  $j_y = \kappa_e (E_y - v_x B_z) \simeq \kappa_e E_0$ .]

If the strength of the magnetic field is increased sufficiently, then the magnetic force will dominate the viscous force, except in thin boundary layers near the walls. Outside the boundary layers, in the bulk of the flow, the velocity will adjust so that the electric field vanishes in the rest frame of the fluid (i.e.,  $v_x = E_0/B_0$ ). In the boundary layers  $v_x$  drops sharply from  $E_0/B_0$  to zero at the walls, and correspondingly, a strong viscous force  $\eta \nabla^2 \mathbf{v}$  develops. Since the pressure gradient  $\nabla P$  must be essentially the same in the boundary layer as in the adjacent bulk flow and thus cannot balance this

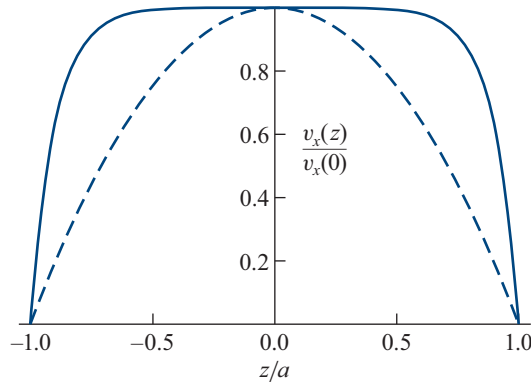


**FIGURE 19.9** Velocity profiles [Eq. (19.35)] for flow in an electromagnetic pump of width  $2a$  with small and large Hartmann number scaled to the velocity at the center of the channel. The dashed curve shows the almost parabolic profile for  $\text{Ha} = 0.1$  [Eq. (19.31)]. The solid curve shows the almost flat-topped profile for  $\text{Ha} = 10$ .

large viscous force, it must be balanced instead by the magnetic force:  $\mathbf{j} \times \mathbf{B} + \eta \nabla^2 \mathbf{v} = 0$  [Eq. (19.30)], with  $\mathbf{j} = \kappa_e(\mathbf{E} + \mathbf{v} \times \mathbf{B}) \sim \kappa_e v_x B_0 \mathbf{e}_y$ . We thereby see that the thickness of the boundary layer is given by

$$\delta_H \sim \left( \frac{\eta}{\kappa_e B_0^2} \right)^{1/2}. \quad (19.32)$$

This suggests a new dimensionless number to characterize the flow,

$$\boxed{\text{Ha} = \frac{a}{\delta_H} = B_0 a \left( \frac{\kappa_e}{\eta} \right)^{1/2}}, \quad (19.33)$$

Hartmann number

called the *Hartmann number*. The square of the Hartmann number,  $\text{Ha}^2$ , is essentially the ratio of the magnetic force,  $|\mathbf{j} \times \mathbf{B}| \sim \kappa_e v_x B_0^2$ , to the viscous force,  $\sim \eta v_x / a^2$ , assuming a lengthscale  $a$  rather than  $\delta_H$  for variations of the velocity.

The detailed velocity profile  $v_x(z)$  away from the vertical side walls is computed in Ex. 19.10 and is shown for low and high Hartmann numbers in Fig. 19.9. Notice that at low Hartmann numbers, the plotted profile is nearly parabolic as expected, and at high Hartmann numbers it consists of boundary layers at  $z \sim -a$  and  $z \sim a$ , and a uniform flow in between.

In Exs. 19.11 and 19.12 we explore two important astrophysical examples of hydro-magnetic flow: the magnetosphere of a rotating, magnetized star or other body, and the solar wind.

## EXERCISES

### Exercise 19.10 Example: Hartmann Flow

Compute the velocity profile of a conducting fluid in a duct of thickness  $2a$  perpendicular to externally generated, uniform electric and magnetic fields ( $E_0 \mathbf{e}_y$ ,

and  $B_0\mathbf{e}_z$ ) as shown in Fig. 19.7. Away from the vertical sides of the duct, the velocity  $v_x$  is just a function of  $z$ , and the pressure can be written in the form  $P = -Qx + p(z)$ , where  $Q$  is the longitudinal pressure gradient.

(a) Show that the velocity field satisfies the differential equation

$$\frac{d^2v_x}{dz^2} - \frac{\kappa_e B_0^2}{\eta} v_x = -\frac{(Q + \kappa_e B_0 E_0)}{\eta}. \quad (19.34)$$

(b) Impose suitable boundary conditions at the bottom and top walls of the channel, and solve this differential equation to obtain the following velocity field:

$$v_x = \frac{Q + \kappa_e B_0 E_0}{\kappa_e B_0^2} \left[ 1 - \frac{\cosh(\text{Ha } z/a)}{\cosh(\text{Ha})} \right], \quad (19.35)$$

where  $\text{Ha}$  is the Hartmann number (see Fig. 19.9).

### Exercise 19.11 *\*\*Example: Rotating Magnetospheres*

Many self-gravitating cosmic bodies are both spinning and magnetized. Examples are Earth, the Sun, black holes surrounded by highly conducting accretion disks (which hold a magnetic field on the hole), neutron stars (pulsars), and magnetic white dwarfs. As a consequence of the magnetic field's spin-induced motion, large electric fields are produced outside the rotating body. The divergence of these electric fields must be balanced by free electric charge, which implies that the region around the body cannot be a vacuum. It is usually filled with plasma and is called a *magnetosphere*. MHD provides a convenient formalism for describing the structure of this magnetosphere. Magnetospheres are found around most planets and stars. Magnetospheres surrounding neutron stars and black holes are believed to be responsible for the emissions from pulsars and quasars.

As a model of a rotating magnetosphere, consider a magnetized and infinitely conducting star, spinning with angular frequency  $\Omega_*$ . Suppose that the magnetic field is stationary and axisymmetric with respect to the spin axis and that the magnetosphere, like the star, is perfectly conducting.

(a) Show that the azimuthal component  $E_\phi$  of the magnetospheric electric field must vanish if the magnetic field is to be stationary. Hence show that there exists a function  $\mathbf{\Omega}(\mathbf{r})$  that must be parallel to  $\mathbf{\Omega}_*$  and must satisfy

$$\mathbf{E} = -(\mathbf{\Omega} \times \mathbf{r}) \times \mathbf{B}. \quad (19.36)$$

Show that if the motion of the magnetosphere's conducting fluid is simply a rotation, then its angular velocity must be  $\mathbf{\Omega}$ .

(b) Use the induction equation (magnetic-field transport law) to show that

$$(\mathbf{B} \cdot \nabla)\mathbf{\Omega} = 0. \quad (19.37)$$

- (c) Use the boundary condition at the surface of the star to show that the magnetosphere corotates with the star (i.e.,  $\mathbf{\Omega} = \mathbf{\Omega}_*$ ). This is known as *Ferraro's law of isorotation*.

**Exercise 19.12** *Example: Solar Wind*

The solar wind is a magnetized outflow of plasma that emerges from the solar corona. We make a simple model of it by generalizing the results from the previous exercise that emphasize its hydromagnetic features while ignoring gravity and thermal pressure (which are also important in practice). We consider stationary, axisymmetric motion in the equatorial plane, and idealize the magnetic field as having the form  $B_r(r)$ ,  $B_\phi(r)$ . (If this were true at all latitudes, the Sun would have to contain magnetic monopoles!)

- (a) Use the results from the previous exercise plus the perfect MHD relation,  $\mathbf{E} = -\mathbf{v} \times \mathbf{B}$ , to argue that the velocity field can be written in the form

$$\mathbf{v} = \frac{\kappa \mathbf{B}}{\rho} + (\mathbf{\Omega} \times \mathbf{r}), \quad (19.38)$$

where  $\kappa$  and  $\mathbf{\Omega}$  are constant along a field line. Interpret this relation kinematically.

- (b) Resolve the velocity and the magnetic field into radial and azimuthal components,  $v_r$ ,  $v_\phi$ , and  $B_r$ ,  $B_\phi$ , and show that  $\rho v_r r^2$  and  $B_r r^2$  are constant.  
 (c) Use the induction equation to show that

$$\frac{v_r}{v_\phi - \Omega r} = \frac{B_r}{B_\phi}. \quad (19.39)$$

- (d) Use the equation of motion to show that the specific angular momentum, including both the mechanical and the magnetic contributions,

$$\Lambda = r v_\phi - \frac{r B_r B_\phi}{\mu_0 \rho v_r}, \quad (19.40)$$

is constant.

- (e) Combine Eqs. (19.39) and (19.40) to argue that

$$v_\phi = \frac{\Omega r [M_A^2 \Lambda / (\Omega r^2) - 1]}{M_A^2 - 1}, \quad (19.41)$$

where

$$M_A = \frac{v_r (\mu_0 \rho)^{1/2}}{B_r} \quad (19.42)$$

is the Alfvén Mach number [cf. Eq. (19.73)]. Show that the solar wind must pass through a critical point (Sec. 17.3.2) where its radial speed equals the Alfvén speed.

- (f) Suppose that the critical point in part (e) is located at 20 solar radii and that  $v_r = 100 \text{ km s}^{-1}$ ,  $v_\phi = 20 \text{ km s}^{-1}$ , and  $B_r = 400 \text{ nT}$  there. Calculate values for  $\Lambda$ ,  $B_\phi$ ,  $\rho$  and use these to estimate the fraction of the solar mass and the solar

angular momentum that could have been carried off by the solar wind over its  $\sim 5$  Gyr lifetime. Comment on your answer.

- (g) Suppose that there is no poloidal current density so that  $B_\phi \propto r^{-1}$ , and deduce values for the velocity and the magnetic field in the neighborhood of Earth where  $r \sim 200$  solar radii. Sketch the magnetic field and the path of the solar wind as it flows from  $r_c$  to Earth.

The solar mass, radius and rotation period are  $\sim 2 \times 10^{30}$  kg,  $\sim 7 \times 10^8$  m, and  $\sim 25$  d.

## 19.5 Stability of Magnetostatic Equilibria

## 19.5

Having used the MHD equation of motion to analyze some simple flows, we return to the problem of magnetic confinement and demonstrate a procedure to analyze the stability of the confinement's magnetostatic equilibria. We first perform a straightforward linear perturbation analysis about equilibrium, obtaining an eigenequation for the perturbation's oscillation frequencies  $\omega$ . For sufficiently simple equilibria, this eigenequation can be solved analytically, but most equilibria are too complex for this approach, so the eigenequation must be solved numerically or by other approximation techniques. This is rather similar to the task one faces in attempting to solve the Schrödinger equation for multi-electron atoms. It will not be a surprise to learn that variational methods are especially practical and useful, and we develop a suitable formalism for them.

We develop the perturbation theory, eigenequation, and variational formalism in some detail not only because of their importance for the stability of magnetostatic equilibria, but also because essentially the same techniques (with different equations) are used in studying the stability of other equilibria. One example is the oscillations and stability of stars, in which the magnetic field is unimportant, while self-gravity is crucial [see, e.g., Shapiro and Teukolsky (1983, Chap. 6), and Sec. 16.2.4 of this book, on helioseismology]. Another example is the oscillations and stability of elastostatic equilibria, in which  $\mathbf{B}$  is absent but shear stresses are important (Secs. 12.3 and 12.4).

### 19.5.1 Linear Perturbation Theory

### 19.5.1

Consider a perfectly conducting, isentropic fluid at rest in equilibrium, with pressure gradients that balance magnetic forces—for example, the Z-pinch,  $\Theta$ -pinch, and tokamak configurations of Fig. 19.6. For simplicity, we ignore gravity. (This is usually justified in laboratory situations.) The equation of equilibrium then reduces to

$$\nabla P = \mathbf{j} \times \mathbf{B} \quad (19.43)$$

[Eq. (19.10)].

equation of magnetostatic equilibrium without gravity

We now perturb slightly about our chosen equilibrium and ignore the (usually negligible) effects of viscosity and magnetic-field diffusion, so  $\eta = \rho\nu \simeq 0$  and  $\kappa_e \simeq \infty$ . It is useful and conventional to describe the perturbations in terms of two different types of quantities: (i) The change in a quantity (e.g., the fluid density) moving with the fluid, which is called a *Lagrangian* perturbation and is denoted by the symbol  $\Delta$  (e.g., the lagrangian density perturbation  $\Delta\rho$ ). (ii) The change at a fixed location in

Lagrangian and Eulerian perturbations and how they are related

space, which is called an *Eulerian* perturbation and is denoted by the symbol  $\delta$  (e.g., the Eulerian density perturbation  $\delta\rho$ ). The fundamental variable used in the theory is the fluid's *Lagrangian displacement*  $\Delta\mathbf{x} \equiv \boldsymbol{\xi}(\mathbf{x}, t)$  (i.e., the change in a fluid element's location). A fluid element whose location is  $\mathbf{x}$  in the unperturbed equilibrium is moved to location  $\mathbf{x} + \boldsymbol{\xi}(\mathbf{x}, t)$  by the perturbations. From their definitions, one can see that the Lagrangian and Eulerian perturbations are related by

$$\Delta = \delta + \boldsymbol{\xi} \cdot \nabla \quad (\text{e.g., } \Delta\rho = \delta\rho + \boldsymbol{\xi} \cdot \nabla\rho). \quad (19.44)$$

Now consider the transport law for the magnetic field in the limit of infinite electrical conductivity,  $\partial\mathbf{B}/\partial t = \nabla \times (\mathbf{v} \times \mathbf{B})$  [Eq. (19.6)]. To linear order, the fluid velocity is  $\mathbf{v} = \partial\boldsymbol{\xi}/\partial t$ . Inserting this into the transport law and setting the full magnetic field at fixed  $\mathbf{x}$  and  $t$  equal to the equilibrium field plus its Eulerian perturbation  $\mathbf{B} \rightarrow \mathbf{B} + \delta\mathbf{B}$ , we obtain  $\partial\delta\mathbf{B}/\partial t = \nabla \times [(\partial\boldsymbol{\xi}/\partial t) \times (\mathbf{B} + \delta\mathbf{B})]$ . Linearizing in the perturbation, and integrating in time, we obtain for the Eulerian perturbation of the magnetic field:

$$\delta\mathbf{B} = \nabla \times (\boldsymbol{\xi} \times \mathbf{B}). \quad (19.45a)$$

Since the current and the field are related, in general, by the linear equation  $\mathbf{j} = \nabla \times \mathbf{B}/\mu_0$ , their Eulerian perturbations are related in the same way:

$$\delta\mathbf{j} = \nabla \times \delta\mathbf{B}/\mu_0. \quad (19.45b)$$

In the equation of mass conservation,  $\partial\rho/\partial t + \nabla \cdot (\rho\mathbf{v}) = 0$ , we replace the density by its equilibrium value plus its Eulerian perturbation,  $\rho \rightarrow \rho + \delta\rho$ , and replace  $\mathbf{v}$  by  $\partial\boldsymbol{\xi}/\partial t$ . We then linearize in the perturbation to obtain

$$\delta\rho + \rho\nabla \cdot \boldsymbol{\xi} + \boldsymbol{\xi} \cdot \nabla\rho = 0. \quad (19.45c)$$

The Lagrangian density perturbation, obtained from this via Eq. (19.44), is

$$\Delta\rho = -\rho\nabla \cdot \boldsymbol{\xi}. \quad (19.45d)$$

We assume that, as it moves, the fluid gets compressed or expanded adiabatically (no Ohmic or viscous heating, or radiative cooling). Then the Lagrangian change of pressure  $\Delta P$  in each fluid element (moving with the fluid) is related to the Lagrangian change of density by

$$\Delta P = \left( \frac{\partial P}{\partial \rho} \right)_s \Delta\rho = \frac{\gamma P}{\rho} \Delta\rho = -\gamma P \nabla \cdot \boldsymbol{\xi}, \quad (19.45e)$$

where  $\gamma$  is the fluid's adiabatic index (ratio of specific heats), which might or might not be independent of position in the equilibrium configuration. Correspondingly, the Eulerian perturbation of the pressure (perturbation at fixed location) is

$$\delta P = \Delta P - (\boldsymbol{\xi} \cdot \nabla)P = -\gamma P(\nabla \cdot \boldsymbol{\xi}) - (\boldsymbol{\xi} \cdot \nabla)P. \quad (19.45f)$$

This is the pressure perturbation that appears in the fluid's equation of motion.

By replacing  $\mathbf{v} \rightarrow \partial \boldsymbol{\xi} / \partial t$ ,  $P \rightarrow P + \delta P$ ,  $\mathbf{B} \rightarrow \mathbf{B} + \delta \mathbf{B}$ , and  $\mathbf{j} \rightarrow \mathbf{j} + \delta \mathbf{j}$  in the fluid's equation of motion (19.10) and neglecting gravity, and by then linearizing in the perturbation, we obtain

$$\rho \frac{\partial^2 \boldsymbol{\xi}}{\partial t^2} = \mathbf{j} \times \delta \mathbf{B} + \delta \mathbf{j} \times \mathbf{B} - \nabla \delta P \equiv \hat{\mathbf{F}}[\boldsymbol{\xi}]. \quad (19.46)$$

dynamical equation for adiabatic perturbations of a magnetostatic equilibrium

Here  $\hat{\mathbf{F}}$  is a real, linear differential operator, whose form one can deduce by substituting expressions (19.45a), (19.45b), and (19.45f) for  $\delta \mathbf{B}$ ,  $\delta \mathbf{j}$ , and  $\delta P$ , and by substituting  $\nabla \times \mathbf{B} / \mu_0$  for  $\mathbf{j}$ . Performing these substitutions and carefully rearranging the terms, we eventually convert the operator  $\hat{\mathbf{F}}$  into the following form, expressed in slot-naming index notation:

$$\hat{F}_i[\boldsymbol{\xi}] = \left\{ \left[ (\gamma - 1)P + \frac{B^2}{2\mu_0} \right] \zeta_{k;k} + \frac{B_j B_k}{\mu_0} \zeta_{j;k} \right\}_{;i} + \left[ \left( P + \frac{B^2}{2\mu_0} \right) \zeta_{j;i} + \frac{B_j B_k}{\mu_0} \zeta_{i;k} + \frac{B_i B_j}{\mu_0} \zeta_{k;k} \right]_{;j}. \quad (19.47)$$

Honestly! Here the semicolons denote gradients (partial derivatives in Cartesian coordinates; connection coefficients (Sec. 11.8) are required in curvilinear coordinates).

We write the operator  $\hat{F}_i$  in the explicit form (19.47) because of its power for demonstrating that  $\hat{F}_i$  is self-adjoint (Hermitian, with real variables rather than complex): by introducing the Kronecker-delta components of the metric,  $g_{ij} = \delta_{ij}$ , we can easily rewrite Eq. (19.47) in the form

$$\hat{F}_i[\boldsymbol{\xi}] = (T_{ijkl} \zeta_{k;l})_{;j}, \quad (19.48)$$

where  $T_{ijkl}$  are the components of a fourth-rank tensor that is symmetric under interchange of its first and second pairs of indices:  $T_{ijkl} = T_{klij}$ .

Now, our magnetic-confinement equilibrium configuration (e.g., Fig. 19.6) typically consists of a plasma-filled interior region  $\mathcal{V}$  surrounded by a vacuum magnetic field (which in turn may be surrounded by a wall). Our MHD equations with force operator  $\hat{\mathbf{F}}$  are valid only in the plasma region  $\mathcal{V}$ , and not in vacuum, where Maxwell's equations with small displacement current prevail. We use Eq. (19.48) to prove that  $\hat{\mathbf{F}}$  is a self-adjoint operator when integrated over  $\mathcal{V}$ , with the appropriate boundary conditions at the vacuum interface.

Specifically, we contract a vector field  $\boldsymbol{\zeta}$  into  $\hat{\mathbf{F}}[\boldsymbol{\xi}]$ , integrate over  $\mathcal{V}$ , and perform two integrations by parts to obtain

$$\begin{aligned} \int_{\mathcal{V}} \boldsymbol{\zeta} \cdot \mathbf{F}[\boldsymbol{\xi}] dV &= \int_{\mathcal{V}} \zeta_i (T_{ijkl} \zeta_{k;l})_{;j} dV = - \int_{\mathcal{V}} T_{ijkl} \zeta_{i;j} \zeta_{k;l} dV = \int_{\mathcal{V}} \zeta_i (T_{ijkl} \zeta_{k;l})_{;j} dV \\ &= \int_{\mathcal{V}} \boldsymbol{\xi} \cdot \mathbf{F}[\boldsymbol{\zeta}] dV. \end{aligned} \quad (19.49)$$

force operator  $\hat{F}_i[\boldsymbol{\xi}]$  is self-adjoint

Here we have discarded the integrals of two divergences, which by Gauss's theorem can be expressed as surface integrals at the fluid-vacuum interface  $\partial\mathcal{V}$ . Those unwanted surface integrals vanish if  $\xi$  and  $\zeta$  satisfy

$$T_{ijkl}\xi_{k;l}\zeta_in_j = 0, \quad \text{and} \quad T_{ijkl}\zeta_{k;l}\xi_in_j = 0, \quad (19.50)$$

with  $n_j$  the normal to the interface  $\partial\mathcal{V}$ .

boundary conditions for perturbations

Now,  $\xi$  and  $\zeta$  are physical displacements of the MHD fluid, and as such, they must satisfy the appropriate boundary conditions at the boundary  $\partial\mathcal{V}$  of the plasma region  $\mathcal{V}$ . In the simplest, idealized case, the conducting fluid would extend far beyond the region where the disturbances have appreciable amplitude, so  $\xi = \zeta = 0$  at the distant boundary, and Eqs. (19.50) are satisfied. More reasonably, the fluid might butt up against rigid walls at  $\partial\mathcal{V}$ , where the normal components of  $\xi$  and  $\zeta$  vanish, guaranteeing again that Eqs. (19.50) are satisfied. This configuration is fine for liquid mercury or sodium, but not for a hot plasma, which would quickly destroy the walls. For confinement by a surrounding vacuum magnetic field, no current flows outside  $\mathcal{V}$ , and the displacement current is negligible, so  $\nabla \times \delta\mathbf{B} = 0$  there. By combining this with the rest of Maxwell's equations and paying careful attention to the motion of the interface and boundary conditions [Eqs. (19.20)] there, one can show, once again, that Eqs. (19.50) are satisfied (see, e.g., Goedbloed and Poedts, 2004, Sec. 6.6.2). Therefore, in all these cases Eq. (19.49) is also true, which demonstrates the self-adjointness (Hermiticity) of  $\hat{\mathbf{F}}$ .<sup>5</sup> We use this property below.

Returning to our perturbed MHD system, we seek its normal modes by assuming a harmonic time dependence,  $\xi \propto e^{-i\omega t}$ . The first-order equation of motion (19.46) then becomes

Sturm-Liouville type eigenequation for perturbations

$$\hat{\mathbf{F}}[\xi] + \rho\omega^2\xi = 0. \quad (19.51)$$

This is an eigenequation for the fluid's Lagrangian displacement  $\xi$ , with eigenvalue  $\omega^2$ . It must be augmented by the boundary conditions (19.20) at the edge  $\partial\mathcal{V}$  of the fluid.

properties of eigenfrequencies and eigenfunctions

By virtue of the elegant, self-adjoint mathematical form (19.48) of the differential operator  $\hat{\mathbf{F}}$ , our eigenequation (19.51) is of a very special and powerful type, called *Sturm-Liouville*; see any good text on mathematical physics (e.g., Mathews and Walker, 1970; Arfken, Weber, and Harris, 2013; Hassani, 2013). From the general (rather simple) theory of Sturm-Liouville equations, we can infer that all the eigenvalues  $\omega^2$  are real, so the normal modes are purely oscillatory ( $\omega^2 > 0$ ,  $\xi \propto e^{\pm i|\omega|t}$ ) or are purely exponentially growing or decaying ( $\omega^2 < 0$ ,  $\xi \propto e^{\pm|\omega|t}$ ). Exponentially growing modes represent instabilities. Sturm-Liouville theory also implies that all

5. Self-adjointness can also be deduced from energy conservation without getting entangled in detailed boundary conditions (see, e.g., Bellan, 2006, Sec. 10.4.2).

eigenfunctions [labeled by indices “(n)”] with different eigenfrequencies are orthogonal to one another, in the sense that  $\int_V \rho \xi^{(n)} \cdot \xi^{(m)} dV = 0$ .

## EXERCISES

### Exercise 19.13 *Derivation: Properties of Eigenmodes*

Derive the properties of the eigenvalues and eigenfunctions for perturbations of an MHD equilibrium that are asserted in the last paragraph of Sec. 19.5.1, namely, the following.

- (a) For each normal mode the eigenfrequency  $\omega_n$  is either real or imaginary.
- (b) Eigenfunctions  $\xi^{(m)}$  and  $\xi^{(n)}$  that have different eigenvalues  $\omega_m \neq \omega_n$  are orthogonal to each other:  $\int \rho \xi^{(m)} \cdot \xi^{(n)} dV = 0$ .

### 19.5.2 Z-Pinch: Sausage and Kink Instabilities

19.5.2

We illustrate MHD stability theory using a simple, analytically tractable example: a variant of the Z-pinch configuration of Fig. 19.6a. We consider a long, cylindrical column of a conducting, incompressible liquid (e.g., mercury) with column radius  $R$  and fluid density  $\rho$ . The column carries a current  $I$  longitudinally along its surface (rather than in its interior as in Fig. 19.6a), so  $\mathbf{j} = [I/(2\pi R)]\delta(\varpi - R)\mathbf{e}_z$ , and the liquid is confined by the resulting external toroidal magnetic field  $B_\phi \equiv B$ . The interior of the plasma is field free and at constant pressure  $P_0$ . From  $\nabla \times \mathbf{B} = \mu_0 \mathbf{j}$ , we deduce that the exterior magnetic field is

$$B_\phi \equiv B = \frac{\mu_0 I}{2\pi \varpi} \quad \text{at } \varpi \geq R. \quad (19.52)$$

Here  $(\varpi, \phi, z)$  are the usual cylindrical coordinates. This is a variant of the Z-pinch, because the  $z$ -directed current on the column's surface creates the external toroidal field  $B$ , which pinches the column until its internal pressure is balanced by the field's pressure:

$$P_0 = \left( \frac{B^2}{2\mu_0} \right)_{\varpi=R}. \quad (19.53)$$

It is quicker and more illuminating to analyze the stability of this Z-pinch equilibrium directly instead of by evaluating  $\hat{\mathbf{F}}$ , and the outcome is the same. (For a treatment based on  $\hat{\mathbf{F}}$ , see Ex. 19.16.) Treating only the most elementary case, we consider small, axisymmetric perturbations with an assumed variation  $\xi \propto e^{i(kz - \omega t)} \mathbf{f}(\varpi)$  for some function  $\mathbf{f}$ . As the magnetic field interior to the column vanishes, the equation of motion  $\rho d\mathbf{v}/dt = -\nabla(P + \delta P)$  becomes

$$-\omega^2 \rho \xi_{\varpi\varpi} = -\delta P', \quad -\omega^2 \rho \xi_z = -ik \delta P, \quad (19.54a)$$

where the prime denotes differentiation with respect to radius  $\varpi$ . Combining these two equations, we obtain

$$\xi_z' = ik \xi_{\varpi}. \quad (19.54b)$$

Because the fluid is incompressible, it satisfies  $\nabla \cdot \xi = 0$ :

$$\varpi^{-1}(\varpi \zeta_\varpi)' + ik\zeta_z = 0, \quad (19.54c)$$

which, with Eq. (19.54b), leads to

$$\zeta_z'' + \frac{\zeta_z'}{\varpi} - k^2\zeta_z = 0. \quad (19.54d)$$

The solution of this equation that is regular at  $\varpi = 0$  is

$$\zeta_z = AI_0(k\varpi) \quad \text{at } \varpi \leq R, \quad (19.54e)$$

where  $A$  is a constant, and  $I_n(x)$  is the modified Bessel function:  $I_n(x) = i^{-n}J_n(ix)$ . From Eq. (19.54b) and  $dI_0(x)/dx = I_1(x)$ , we obtain

$$\zeta_\varpi = -iAI_1(k\varpi). \quad (19.54f)$$

Next we consider the region exterior to the fluid column. As this is vacuum, it must be current free; and as we are dealing with a purely axisymmetric perturbation, the  $\varpi$  component of Maxwell's equation  $\nabla \times \delta\mathbf{B} = 0$  (with negligible displacement current) reads

$$\frac{\partial \delta B_\phi}{\partial z} = ik\delta B_\phi = 0. \quad (19.54g)$$

The  $\phi$  component of the magnetic perturbation therefore vanishes outside the column.

The interior and exterior solutions must be connected by the law of force balance, that is, by the boundary condition (19.19f) [or equivalently, Eq. (19.20a) with the tildes removed] at the plasma's surface. Allowing for the displacement of the surface and retaining only linear terms, this becomes

$$P_0 + \Delta P = P_0 + (\xi \cdot \nabla)P_0 + \delta P = \frac{(B + \Delta B_\phi)^2}{2\mu_0} = \frac{B^2}{2\mu_0} + \frac{B}{\mu_0}(\xi \cdot \nabla)B + \frac{B\delta B_\phi}{\mu_0}, \quad (19.54h)$$

where all quantities are evaluated at  $\varpi = R$ . The equilibrium force-balance condition gives us  $P_0 = B^2/(2\mu_0)$  [Eq. (19.53)] and  $\nabla P_0 = 0$ . In addition, we have shown that  $\delta B_\phi = 0$ . Therefore, Eq. (19.54h) becomes simply

$$\delta P = \frac{BB'}{\mu_0}\zeta_\varpi. \quad (19.54i)$$

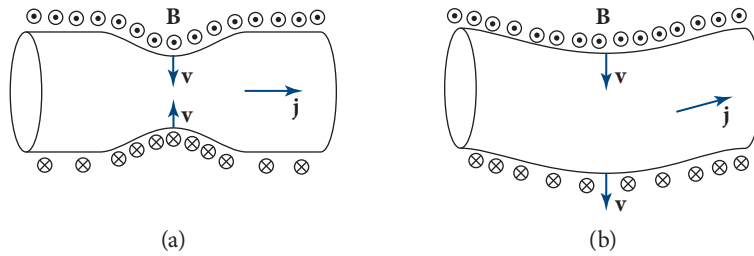


FIGURE 19.10 Physical interpretation of (a) sausage and (b) kink instabilities.

Substituting  $\delta P$  from Eqs. (19.54a) and (19.54e),  $B$  from Eq. (19.52), and  $\xi_{\varpi}$  from Eq. (19.54f), we obtain the dispersion relation

$$\begin{aligned}\omega^2 &= \frac{-\mu_0 I^2}{4\pi^2 R^4 \rho} \frac{k R I_1(kR)}{I_0(kR)} \\ &\simeq \frac{-\mu_0 I^2}{8\pi^2 R^2 \rho} k^2; \quad \text{for } k \ll R^{-1} \\ &\simeq \frac{-\mu_0 I^2}{4\pi^2 R^3 \rho} k; \quad \text{for } k \gg R^{-1},\end{aligned}\quad (19.55)$$

where we have used  $I_0(x) \sim 1$ ,  $I_1(x) \sim x/2$  as  $x \rightarrow 0$  and  $I_1(x)/I_0(x) \rightarrow 1$  as  $x \rightarrow \infty$ .

Because  $I_0$  and  $I_1$  are positive for all  $kR > 0$ , for every wave number  $k$  this dispersion relation shows that  $\omega^2$  is negative. Therefore,  $\omega$  is imaginary, the perturbation grows exponentially with time, and so *the Z-pinch configuration is dynamically unstable*. If we define a characteristic Alfvén speed by  $a = B(R)/(\mu_0 \rho)^{1/2}$  [see Eq. (19.73)], then we see that the growth time for modes with wavelengths comparable to the column diameter is roughly an Alfvén crossing time  $2R/a$ . This is fast!

This instability is sometimes called a *sausage instability*, because its eigenfunction  $\xi_{\varpi} \propto e^{ikz}$  consists of oscillatory pinches of the column’s radius that resemble the pinches between sausages in a link. This sausage instability has a simple physical interpretation (Fig. 19.10a), one that illustrates the power of the concepts of flux freezing and magnetic tension for developing intuition. If we imagine an inward radial motion of the fluid, then the toroidal loops of magnetic field will be carried inward, too, and will therefore shrink. As the external field is unperturbed,  $\delta B_{\phi} = 0$ , we have  $B_{\phi} \propto 1/\varpi$ , whence the surface field at the inward perturbation increases, leading to a larger “hoop” stress or, equivalently, a larger  $\mathbf{j} \times \mathbf{B}$  Lorentz force, which accelerates the inward perturbation (see Fig. 19.10a).

So far, we have only considered axisymmetric perturbations. We can generalize our analysis by allowing the perturbations to vary as  $\xi \propto \exp(im\phi)$ . (Our sausage instability corresponds to  $m = 0$ .) Modes with  $m \geq 1$ , like  $m = 0$ , are also generically unstable. The  $m = 1$  modes are known as *kink* modes. In this case the column bends,

sausage instability of Z-pinch

kink instability of Z-pinch

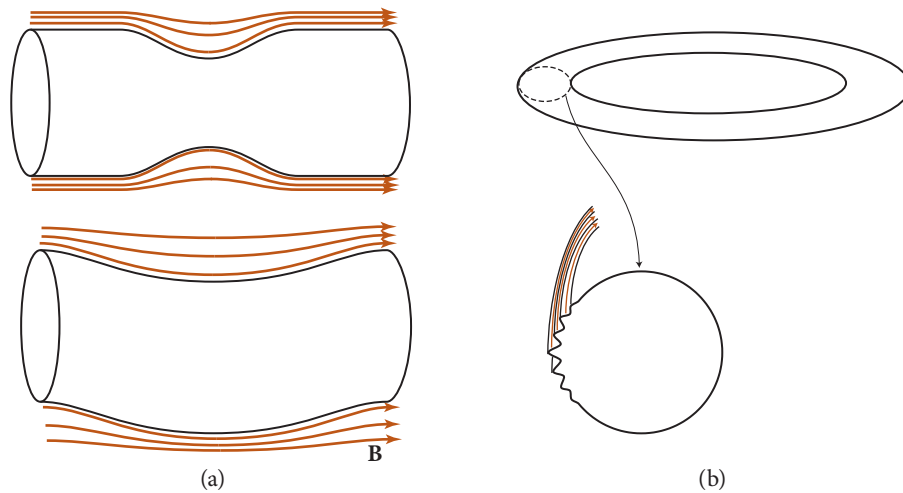


FIGURE 19.11 (a) Stabilizing magnetic fields for  $\Theta$ -pinch configuration. (b) Flute instability for  $\Theta$ -pinch configuration made into a torus.

and the field strength is intensified along the inner face of the bend and reduced on the outer face, thereby amplifying the instability (Fig. 19.10b). The incorporation of compressibility, as is appropriate for plasma instead of mercury, introduces only algebraic complexity; the conclusions are unchanged. The column is still highly unstable. It remains so if we distribute the longitudinal current throughout the column's interior, thereby adding a magnetic field to the interior, as in Fig. 19.6a. MHD instabilities such as these have bedeviled attempts to confine plasma long enough to bring about nuclear fusion. Indeed, considerations of MHD stability were one of the primary motivations for the tokamak, the most consistently successful of experimental fusion devices.

### 19.5.3

#### 19.5.3 The $\Theta$ -Pinch and Its Toroidal Analog; Flute Instability; Motivation for Tokamak

full stability of  $\Theta$ -pinch

By contrast with the extreme instability of the Z-pinch configuration, the  $\Theta$ -pinch configuration (Sec. 19.3.3 and Fig. 19.6b) is fully stable against MHD perturbations! (See Ex. 19.14.) This is easily understood physically (Fig. 19.11a). When the plasma cylinder is pinched or bent, at outward displaced regions of the cylinder, the external longitudinal magnetic field lines are pushed closer together, thereby strengthening the magnetic field and its pressure and thence creating an inward restoring force. Similarly, at inward displaced regions, the field lines are pulled apart, weakening their pressure and creating an outward restoring force.

Unfortunately, the  $\Theta$ -pinch configuration cannot confine plasma without closing its ends. The ends can be partially closed by a pair of magnetic mirrors, but there remain losses out the ends that cause problems. The ends can be fully closed by bending the column into a closed torus, but, sadly, the resulting toroidal  $\Theta$ -pinch configuration exhibits a new MHD “flute” instability (Fig. 19.11b).

toroidal  $\Theta$ -pinch: flute instability

This flute instability arises on and near the outermost edge of the torus. That edge is curved around the torus's symmetry axis in just the same way as the face of the Z-pinch configuration is curved around its symmetry axis—with the magnetic field in both cases forming closed loops around the axis. As a result, this outer edge is subject to a sausage-type instability, similar to that of the Z-pinch. The resulting corrugations are translated along the torus, so they resemble the flutes on a Greek column that supports an architectural arch or roof (hence the name “flute instability”). This fluting can also be understood as a flux-tube interchange instability (Ex. 19.15).

The flute instability can be counteracted by endowing the torus with an internal magnetic field that twists (shears) as one goes radially inward (the tokamak configuration of Fig. 19.6c). Adjacent magnetic surfaces (isobars), with their different field directions, counteract each other's MHD instabilities. The component of the magnetic field along the plasma torus provides a pressure that stabilizes against sausage instabilities and a tension that stabilizes against kink-type instabilities; the component around the torus's guiding circle acts to stabilize its flute modes. In addition, the formation of image currents in the conducting walls of a tokamak vessel can also have a stabilizing influence.

how tokamak configuration counteracts instabilities

**Exercise 19.14** *Problem and Challenge: Stability of  $\Theta$ -Pinch*

Derive the dispersion relation  $\omega^2(k)$  for axisymmetric perturbations of the  $\Theta$ -pinch configuration when the magnetic field is confined to the cylinder's exterior, and conclude from it that the  $\Theta$ -pinch is stable against axisymmetric perturbations. [Hint: The analysis of the interior of the cylinder is the same as for the Z-pinch analyzed in the text.] Repeat your analysis for a general, variable-separated perturbation of the form  $\xi \propto e^{i(m\theta + kz - \omega t)}$ , and thereby conclude that the  $\Theta$ -pinch is fully MHD stable.

**Exercise 19.15** *Example: Flute Instability Understood by Flux-Tube Interchange*

Carry out an analysis of the flute instability patterned after that for rotating Couette flow (first long paragraph of Sec. 14.6.3) and that for convection in stars (Fig. 18.5): Imagine exchanging two plasma-filled magnetic flux tubes that reside near the outermost edge of the torus. Argue that the one displaced outward experiences an unbalanced outward force, and the one displaced inward experiences an unbalanced inward force. [Hint: (i) To simplify the analysis, let the equilibrium magnetic field rise from zero continuously in the outer layers of the torus rather than arising discontinuously at its surface, and consider flux tubes in that outer, continuous region. (ii) Argue that the unbalanced force per unit length on a displaced flux tube is  $[-\nabla(P + B^2/(2\mu_0)) - (B_{\text{tube}}^2/\varpi)\mathbf{e}_\varpi]A$ . Here  $A$  is the tube's cross sectional area,  $\varpi$  is distance from the torus's symmetry axis,  $\mathbf{e}_\varpi$  is the unit vector pointing away from the symmetry axis,  $B_{\text{tube}}$  is the field strength inside the displaced tube, and  $\nabla(P + B^2/(2\mu_0))$  is the net surrounding pressure gradient at the tube's

**EXERCISES**

displaced location.] Argue further that the innermost edge of the torus is stable against flux-tube interchange, so the flute instability is confined to the torus's outer face.

#### 19.5.4 19.5.4 Energy Principle and Virial Theorems T2

For the perturbation eigenequation (19.46) and its boundary conditions, analytical or even numerical solutions are only readily obtained in the most simple of geometries and for the simplest fluids. However, as the eigenequation is self-adjoint, it is possible to write down a variational principle and use it to derive approximate stability criteria. This variational principle has been a powerful tool for analyzing the stability of tokamak and other magnetostatic configurations.

To derive the variational principle, we begin by multiplying the fluid velocity  $\dot{\xi} = \partial\xi/\partial t$  into the eigenequation (equation of motion)  $\rho\partial^2\xi/\partial t^2 = \hat{F}[\xi]$ . We then integrate over the plasma-filled region  $\mathcal{V}$ , and use the self-adjointness of  $\hat{F}$  to write  $\int_{\mathcal{V}} dV \dot{\xi} \cdot \hat{F}[\xi] = \frac{1}{2} \int_{\mathcal{V}} dV (\dot{\xi} \cdot \hat{F}[\xi] + \xi \cdot \hat{F}[\dot{\xi}])$ . We thereby obtain

$$\frac{dE}{dt} = 0, \quad \text{where } E = T + W, \quad (19.56a)$$

$$T = \int_{\mathcal{V}} dV \frac{1}{2} \rho \dot{\xi}^2, \quad \text{and} \quad W = W[\xi] \equiv -\frac{1}{2} \int_{\mathcal{V}} dV \xi \cdot \hat{F}[\xi]. \quad (19.56b)$$

The integrals  $T$  and  $W$  are the perturbation's kinetic and potential energy, and  $E = T + W$  is the conserved total energy.

Any solution of the equation of motion  $\partial^2\xi/\partial t^2 = \hat{F}[\xi]$  can be expanded in terms of a complete set of normal modes  $\xi^{(n)}(\mathbf{x})$  with eigenfrequencies  $\omega_n$ :  $\xi = \sum_n A_n \xi^{(n)} e^{-i\omega_n t}$ . Because  $\hat{F}$  is a real, self-adjoint operator, these normal modes can all be chosen to be real and orthogonal, even when some of their frequencies are degenerate. As the perturbation evolves, its energy sloshes back and forth between kinetic  $T$  and potential  $W$ , so time averages of  $T$  and  $W$  are equal:  $\overline{T} = \overline{W}$ . This implies, for each normal mode,

$$\omega_n^2 = \frac{W[\xi^{(n)}]}{\int_{\mathcal{V}} dV \frac{1}{2} \rho \xi^{(n)2}}. \quad (19.57)$$

As the denominator is positive definite, we conclude that *a magnetostatic equilibrium is stable against small perturbations if and only if the potential energy  $W[\xi]$  is a positive-definite functional of the perturbation  $\xi$* . This is sometimes called the *Rayleigh principle* for a general Sturm-Liouville problem. In the MHD context, it is known as the *energy principle*.

It is straightforward to verify, by virtue of the self-adjointness of  $\hat{F}[\xi]$ , that expression (19.57) serves as an action principle for the eigenfrequencies: If one inserts into Eq. (19.57) a trial function  $\xi_{\text{trial}}$  in place of  $\xi^{(n)}$ , then the resulting value of the equation will be stationary under small variations of  $\xi_{\text{trial}}$  if and only if  $\xi_{\text{trial}}$  is equal to

conserved energy for adiabatic perturbations of magnetostatic configurations

energy principle (Rayleigh principle) for stability

action principle for eigenfrequencies

some eigenfunction  $\xi^{(n)}$ ; and the stationary value of Eq. (19.57) is that eigenfunction's squared eigenfrequency  $\omega_n^2$ . This action principle is most useful for estimating the lowest few squared frequencies  $\omega_n^2$ . Because first-order differences between  $\xi_{\text{trial}}$  and  $\xi^{(n)}$  produce second-order errors in  $\omega_n^2$ , relatively crude trial eigenfunctions can furnish surprisingly accurate eigenvalues.

Whatever may be our chosen trial function  $\xi_{\text{trial}}$ , the computed value of the action (19.57) will always be larger than  $\omega_0^2$ , the squared eigenfrequency of the most unstable mode. Therefore, if we compute a negative value of Eq. (19.57) using some trial eigenfunction, we know that the equilibrium must be even more unstable.

The MHD energy principle and action principle are special cases of the general conservation law and action principle for Sturm-Liouville differential equations (see, e.g., Mathews and Walker, 1970; Arfken, Weber, and Harris, 2013; Hassani, 2013). For further insights into the energy and action principles, see the original MHD paper by Bernstein et al. (1958), in which these ideas were developed; also see Mikhailovskii (1998), Goedbloed and Poedts (2004, Chap. 6), and Bellan (2006, Chap. 10).

## EXERCISES

### Exercise 19.16 *Example: Reformulation of the Energy Principle;*

#### *Application to Z-Pinch* T2

The form of the potential energy functional derived in the text [Eq. (19.47)] is optimal for demonstrating that the operator  $\hat{F}$  is self-adjoint. However, there are several simpler, equivalent forms that are more convenient for practical use.

(a) Use Eq. (19.46) to show that

$$\begin{aligned} \xi \cdot \hat{F}[\xi] = & \mathbf{j} \times \mathbf{b} \cdot \xi - \mathbf{b}^2/\mu_0 - \gamma P(\nabla \cdot \xi)^2 - (\nabla \cdot \xi)(\xi \cdot \nabla)P \\ & + \nabla \cdot [(\xi \times \mathbf{B}) \times \mathbf{b}/\mu_0 + \gamma P \xi(\nabla \cdot \xi) + \xi(\xi \cdot \nabla)P], \end{aligned} \quad (19.58)$$

where  $\mathbf{b} \equiv \delta \mathbf{B}$  is the Eulerian perturbation of the magnetic field.

(b) Insert Eq. (19.58) into expression (19.56b) for the potential energy  $W[\xi]$  and convert the volume integral of the divergence into a surface integral. Then impose the boundary condition of a vanishing normal component of the magnetic field at  $\partial \mathcal{V}$  [Eq. (19.20b)] to show that

$$\begin{aligned} W[\xi] = & \frac{1}{2} \int_{\mathcal{V}} dV \left[ -\mathbf{j} \times \mathbf{b} \cdot \xi + \mathbf{b}^2/\mu_0 + \gamma P(\nabla \cdot \xi)^2 + (\nabla \cdot \xi)(\xi \cdot \nabla)P \right] \\ & - \frac{1}{2} \int_{\partial \mathcal{V}} d\Sigma \cdot \xi \left[ \gamma P(\nabla \cdot \xi) + \xi \cdot \nabla P - \mathbf{B} \cdot \mathbf{b}/\mu_0 \right]. \end{aligned} \quad (19.59)$$

(c) Consider axisymmetric perturbations of the cylindrical Z-pinch of an incompressible fluid, as discussed in Sec. 19.5.2, and argue that the surface integral vanishes.

(d) Adopt a simple trial eigenfunction, and obtain a variational estimate of the growth rate of the sausage instability's fastest growing mode.

T2

**Exercise 19.17** *Problem: Potential Energy in Its Most Physically Interpretable Form* T2

(a) Show that the potential energy (19.59) can be transformed into the following form:

$$W[\xi] = \frac{1}{2} \int_{\mathcal{V}} dV \left[ -\mathbf{j} \times \mathbf{b} \cdot \xi + \frac{\mathbf{b}^2}{\mu_0} + \delta P \frac{\Delta \rho}{\rho} \right] + \frac{1}{2} \int_{\partial V} d\boldsymbol{\Sigma} \cdot \nabla \left( \frac{\tilde{B}^2}{2\mu_0} - P - \frac{B^2}{2\mu_0} \right) \xi_n^2 + \frac{1}{2} \int_{\text{vacuum}} dV \frac{\tilde{\mathbf{b}}^2}{\mu_0}. \quad (19.60)$$

Here symbols without tildes represent quantities in the plasma region, and those with tildes are in the vacuum region;  $\xi_n$  is the component of the fluid displacement orthogonal to the vacuum-plasma interface.

(b) Explain the physical interpretation of each term in the expression for the potential energy in part (a). Notice that, although our original expression for the potential energy,  $W = -\frac{1}{2} \int_{\mathcal{V}} \xi \cdot \mathbf{F}[\xi] dV$ , entails an integral only over the plasma region, it actually includes the vacuum region's magnetic energy.

**Exercise 19.18** *Example: Virial Theorems* T2

Additional mathematical tools that are useful in analyzing MHD equilibria and their stability—and are also useful in astrophysics—are the *virial theorems*. In this exercise and the next, you will deduce time-dependent and time-averaged virial theorems for any system for which the law of momentum conservation can be written in the form

$$\frac{\partial(\rho v_j)}{\partial t} + T_{jk;k} = 0. \quad (19.61)$$

Here  $\rho$  is mass density,  $v_j$  is the material's velocity,  $\rho v_j$  is momentum density, and  $T_{jk}$  is the stress tensor. We have met this formulation of momentum conservation in elastodynamics [Eq. (12.2b)], in fluid mechanics with self-gravity [Eq. (2) of Box 13.4], and in magnetohydrodynamics with self-gravity [Eq. (19.12)].

The virial theorems involve integrals over any region  $\mathcal{V}$  for which there is no mass flux or momentum flux across its boundary:  $\rho v_j n_j = T_{jk} n_k = 0$  everywhere on  $\partial \mathcal{V}$ , where  $n_j$  is the normal to the boundary.<sup>6</sup> For simplicity we use Cartesian coordinates, so there are no connection coefficients to worry about, and momentum conservation becomes  $\partial(\rho v_j) + \partial T_{jk} / \partial x_k = 0$ .

(a) Show that mass conservation,  $\partial \rho / \partial t + \nabla \cdot (\rho \mathbf{v}) = 0$ , implies that for any field  $f$  (scalar, vector, or tensor), we have

$$\frac{d}{dt} \int_{\mathcal{V}} \rho f dV = \int_{\mathcal{V}} \rho \frac{df}{dt} dV. \quad (19.62)$$

6. If self-gravity is included, then the boundary will have to be at spatial infinity (i.e., no boundary), as  $T_{jk}^{\text{grav}} n_k$  cannot vanish everywhere on a finite enclosing wall.

(b) Use Eq. (19.62) to show that

$$\boxed{\frac{d^2 I_{jk}}{dt^2} = 2 \int_{\mathcal{V}} \tau_{jk} dV,} \quad (19.63a)$$

where  $I_{jk}$  is the second moment of the mass distribution:

$$I_{jk} = \int_{\mathcal{V}} \rho x_j x_k dV \quad (19.63b)$$

with  $x_j$  the distance from a chosen origin. This is the *time-dependent tensor virial theorem*. (Note that the system's mass quadrupole moment is the trace-free part of  $I_{jk}$ ,  $\mathcal{I}_{jk} = I_{jk} - \frac{1}{3} I g_{jk}$ , and the system's moment of inertia tensor is  $\mathfrak{J}_{jk} = I_{jk} - I g_{jk}$ , where  $I = I_{jj}$  is the trace of  $I_{jk}$ .)

(c) If the time integral of  $d^2 I_{jk}/dt^2$  vanishes, then the time-averaged stress tensor satisfies

$$\boxed{\int_{\mathcal{V}} \bar{\tau}_{jk} dV = 0.} \quad (19.64)$$

This is the *time-averaged tensor virial theorem*. Under what circumstances is this theorem true?

**Exercise 19.19** Example: Scalar Virial Theorems T2

(a) By taking the trace of the time-dependent tensorial virial theorem and specializing to an MHD plasma with (or without) self-gravity, show that

$$\boxed{\frac{1}{2} \frac{d^2 I}{dt^2} = 2E_{\text{kin}} + E_{\text{mag}} + E_{\text{grav}} + 3E_P,} \quad (19.65a)$$

where  $I$  is the trace of  $I_{jk}$ ,  $E_{\text{kin}}$  is the system's kinetic energy,  $E_{\text{mag}}$  is its magnetic energy,  $E_P$  is the volume integral of its pressure, and  $E_{\text{grav}}$  is its gravitational self-energy:

$$I = \int_{\mathcal{V}} \rho \mathbf{x}^2 dV, \quad E_{\text{kin}} = \int_{\mathcal{V}} \frac{1}{2} \rho \mathbf{v}^2 dV, \quad E_{\text{mag}} = \int \frac{\mathbf{B}^2}{2\mu_0}, \quad E_P = \int_{\mathcal{V}} P dV,$$

$$E_{\text{grav}} = \frac{1}{2} \int_{\mathcal{V}} \rho \Phi = - \int_{\mathcal{V}} \frac{1}{8\pi G} (\nabla \Phi)^2 = - \frac{1}{2} \int_{\mathcal{V}} \int_{\mathcal{V}} G \frac{\rho(\mathbf{x})\rho(\mathbf{x}')}{|\mathbf{x} - \mathbf{x}'|} dV' dV, \quad (19.65b)$$

with  $\Phi$  the gravitational potential energy [cf. Eq. (13.62)].

(b) When the time integral of  $d^2 I/dt^2$  vanishes, then the time average of the right-hand side of Eq. (19.65a) vanishes:

$$\boxed{2\bar{E}_{\text{kin}} + \bar{E}_{\text{mag}} + \bar{E}_{\text{grav}} + 3\bar{E}_P = 0.} \quad (19.66)$$

This is the *time-averaged scalar virial theorem*. Give examples of circumstances in which it holds.

T2

- (c) Equation (19.66) is a continuum analog of the better-known scalar virial theorem,  $2\bar{E}_{\text{kin}} + \bar{E}_{\text{grav}} = 0$ , for a system consisting of particles that interact via their self-gravity—for example, the solar system (see, e.g., Goldstein, Poole, and Safko, 2002, Sec. 3.4).
- (d) As a simple but important application of the time-averaged scalar virial theorem, show—neglecting self-gravity—that it is impossible for internal currents in a plasma to produce a magnetic field that confines the plasma to a finite volume: external currents (e.g., in solenoids) are necessary.
- (e) For applications to the oscillation and stability of self-gravitating systems, see Chandrasekhar (1961, Sec. 118).

## 19.6 19.6 Dynamos and Reconnection of Magnetic Field Lines T2

dynamo

As we have already remarked, the timescale for Earth's magnetic field to decay is estimated to be roughly 1 million years. Since Earth is far older than that, some process inside Earth must be regenerating the magnetic field. This process is known as a *dynamo*. Generally speaking, in a dynamo the motion of the fluid stretches the magnetic field lines, thereby increasing their magnetic energy density, which compensates for the decrease in magnetic energy associated with Ohmic decay. The details of how this happens inside Earth are not well understood. However, some general principles of dynamo action have been formulated, and their application to the Sun is somewhat better understood (Exs. 19.20 and 19.21).

### 19.6.1 19.6.1 Cowling's Theorem T2

It is simple to demonstrate the impossibility of dynamo action in any time-independent, axisymmetric flow. Suppose that there were such a dynamo configuration, and the time-independent, poloidal (meridional) field had—for concreteness—the form sketched in Fig. 19.12. Then there must be at least one neutral point marked  $\mathcal{P}$  (actually a circle about the symmetry axis), where the poloidal field vanishes. However, the curl of the magnetic field does not vanish at  $\mathcal{P}$ , so a toroidal current  $j_\phi$  must exist there. Now, in the presence of finite resistivity, there must also be a toroidal electric field at  $\mathcal{P}$ , since

$$j_\phi = \kappa_e [E_\phi + (\mathbf{v}_P \times \mathbf{B}_P)_\phi] = \kappa_e E_\phi. \quad (19.67)$$

Here  $\mathbf{v}_P$  and  $\mathbf{B}_P$  are the poloidal components of  $\mathbf{v}$  and  $\mathbf{B}$ . The nonzero  $E_\phi$  in turn implies, via  $\nabla \times \mathbf{E} = -\partial \mathbf{B} / \partial t$ , that the amount of poloidal magnetic flux threading the circle at  $\mathcal{P}$  must change with time, violating our original supposition that the magnetic field distribution is stationary.

Cowling's theorem for dynamos

We therefore conclude that any time-independent, self-perpetuating dynamo must be more complicated than a purely axisymmetric magnetic field. This result is known as *Cowling's theorem*.

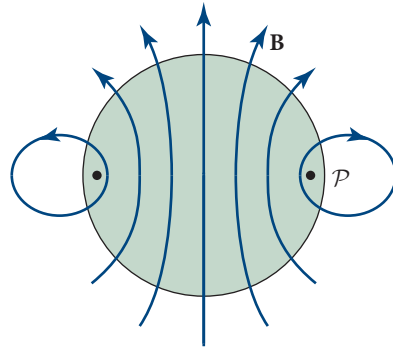


FIGURE 19.12 Impossibility of an axisymmetric dynamo.

### 19.6.2 Kinematic Dynamos T2

19.6.2

The simplest types of dynamo to consider are those in which we specify a particular velocity field and allow the magnetic field to evolve according to the transport law (19.6). Under certain circumstances, this can produce dynamo action. Note that we do not consider in our discussion the dynamical effect of the magnetic field on the velocity field.

The simplest type of motion is one in which a *dynamo cycle* occurs. In this cycle, there is one mechanism for creating a toroidal magnetic field from a poloidal field and a separate mechanism for regenerating the poloidal field. The first mechanism is usually differential rotation. The second is plausibly magnetic buoyancy, in which a toroidal magnetized loop is lighter than its surroundings and therefore rises in the gravitational field. As the loop rises, Coriolis forces twist the flow, causing a poloidal magnetic field to appear, which completes the dynamo cycle.

dynamo cycle

Small-scale, turbulent velocity fields may also be responsible for dynamo action. In this case, it can be shown on general symmetry grounds that the velocity field must contain *hydrodynamic helicity*—a nonzero mean value of  $\mathbf{v} \cdot \boldsymbol{\omega}$  [which is an obvious analog of magnetic helicity (Ex. 19.9), the volume integral or mean value of  $\mathbf{A} \cdot \mathbf{B} = \mathbf{A} \cdot (\nabla \times \mathbf{A})$ ].

dynamo action in turbulence

hydrodynamic helicity

If the magnetic field strength grows, then its dynamical effect will eventually react back on the flow and modify the velocity field. A full description of a dynamo must include this back reaction. Dynamos are a prime target for numerical simulations of MHD, and in recent years, significant progress has been made using these simulations to understand the terrestrial dynamo and other specialized problems.

#### Exercise 19.20 Problem: Differential Rotation in the Solar Dynamo T2

### EXERCISES

This problem shows how differential rotation leads to the production of a toroidal magnetic field from a poloidal field.

- (a) Verify that for a fluid undergoing differential rotation around a symmetry axis with angular velocity  $\Omega(r, \theta)$ , the  $\phi$  component of the induction equation reads

T2

$$\frac{\partial B_\phi}{\partial t} = \sin \theta \left( B_\theta \frac{\partial \Omega}{\partial \theta} + B_r r \frac{\partial \Omega}{\partial r} \right), \quad (19.68)$$

where  $\theta$  is the co-latitude. (The resistive term can be ignored.)

- (b) It is observed that the angular velocity on the solar surface is largest at the equator and decreases monotonically toward the poles. Analysis of solar oscillations (Sec. 16.2.4) has shown that this variation  $\Omega(\theta)$  continues inward through the convection zone (cf. Sec. 18.5). Suppose that the field of the Sun is roughly poloidal. Sketch the appearance of the toroidal field generated by the poloidal field.

**Exercise 19.21** *Problem: Buoyancy in the Solar Dynamo* T2

Consider a slender flux tube with width much less than its length which, in turn, is much less than the external pressure scale height  $H$ . Also assume that the magnetic field is directed along the tube so there is negligible current along the tube.

- (a) Show that the requirement of magnetostatic equilibrium implies that inside the flux tube

$$\nabla \left( P + \frac{B^2}{2\mu_0} \right) \simeq 0. \quad (19.69)$$

- (b) Consider a segment of this flux tube that is horizontal and has length  $\ell$ . Holding both ends fixed, bend it vertically upward so that the radius of curvature of its center line is  $R \gg \ell$ . Assume that the fluid is isentropic with adiabatic index  $\gamma$ . By balancing magnetic tension against buoyancy, show that magnetostatic equilibrium is possible if  $R \simeq 2\gamma H$ . Do you think this equilibrium could be stable?
- (c) In the solar convection zone (cf. Sec. 18.5), small entropy differences are important in driving the convective circulation. Following Ex. 19.20(b), suppose that a length of toroidal field is carried upward by a convecting “blob.” Consider the action of the Coriolis force due to the Sun’s rotation (cf. Sec. 14.2.1) on a single blob, and argue that it will rotate. What will this do to the magnetic field? Sketch the generation of a large-scale poloidal field from a toroidal field through the combined effects of many blobs. What do you expect to observe when a flux tube breaks through the solar surface (known as the photosphere)?

The combined effect of differential rotation, magnetic stress, and buoyancy, as outlined in Exs. 19.20 and 19.21, is thought to play an important role in sustaining the solar dynamo cycle. See Goedbloed and Poedts (2004, Secs. 8.2, 8.3) for further insights.

---

19.6.3 19.6.3 Magnetic Reconnection T2

So far, our discussion of the evolution of the magnetic field has centered on the induction equation (19.6) (the magnetic transport law). We have characterized the

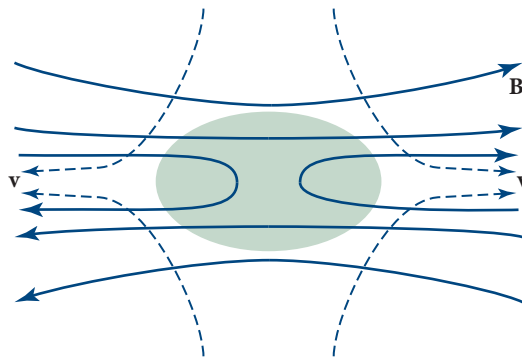


**FIGURE 19.13** Magnetic reconnection. In the shaded reconnection region, Ohmic diffusion is important and allows magnetic field lines to “exchange partners,” changing the overall field topology. Magnetic field components perpendicular to the plane of the illustration do not develop large gradients and so do not inhibit the reconnection process.

magnetized fluid by a magnetic Reynolds number using some characteristic length  $L$  associated with the flow, and have found that, when  $R_M \gg 1$ , Ohmic dissipation and field-line diffusion in the transport law are unimportant. This is reminiscent of the procedure we followed when discussing vorticity. However, for vorticity we discovered a very important exception to an uncritical neglect of viscosity, dissipation, and vortex-line diffusion at large Reynolds numbers, namely, boundary layers (Sec. 14.4). In particular, we found that large-Reynolds-number flows near solid surfaces develop large velocity gradients on account of the no-slip boundary condition, and that the local Reynolds number can thereby decrease to near unity, allowing viscous stress to change the character of the flow completely. Something similar, called *magnetic reconnection*, can happen in hydromagnetic flows with large  $R_M$ , even without the presence of solid surfaces.

Consider two oppositely magnetized regions of conducting fluid moving toward each other (the upper and lower regions in Fig. 19.13). Mutual magnetic attraction of the two regions occurs, as magnetic energy would be reduced if the two sets of field lines were superposed. However, strict flux freezing prevents superposition. Something has to give! What happens is a compromise. The attraction causes large magnetic gradients to develop, accompanied by a buildup of large current densities, until Ohmic diffusion ultimately allows the magnetic field lines to slip sideways through the fluid and to *reconnect* with the field in the other region (the sharply curved field lines in Fig. 19.13).

This reconnection mechanism can be clearly observed at work in tokamaks and in Earth’s magnetopause, where the solar wind’s magnetic field meets Earth’s magnetosphere. However, the details of the reconnection mechanism are quite complex, involving plasma instabilities, anisotropic electrical conductivity, and shock fronts.

how magnetic reconnection occurs at high  $R_M$

T2

Large, inductive electric fields can also develop when the magnetic geometry undergoes rapid change. This can happen in the reversing magnetic field in Earth's *magnetotail*,<sup>7</sup> leading to the acceleration of charged particles that impact Earth during a *magnetic substorm*. Like dynamo action, reconnection has a major role in determining how magnetic fields actually behave in both laboratory and space plasmas.

For further detail on the physics and observations of reconnection, see, for example, Birn and Priest (2007) and Forbes and Priest (2007).

## 19.7

### 19.7 Magnetosonic Waves and the Scattering of Cosmic Rays

magnetosonic waves

In Sec. 19.5, we discussed global perturbations of a nonuniform magnetostatic plasma and described how they may be unstable. We now consider a different, particularly simple example of dynamical perturbations: planar, monochromatic, propagating waves in a uniform, magnetized, conducting medium. These are called *magnetosonic waves*. They can be thought of as sound waves that are driven not just by gas pressure but also by magnetic pressure and tension.

Although magnetosonic waves have been studied experimentally under laboratory conditions, there the magnetic Reynolds numbers are generally quite small, so the waves damp quickly by Ohmic dissipation. No such problem arises in space plasmas, where magnetosonic waves are routinely studied by the many spacecraft that monitor the solar wind and its interaction with planetary magnetospheres. It appears that these modes perform an important function in space plasmas: they control the transport of cosmic rays. Let us describe some properties of cosmic rays before giving a formal derivation of the magnetosonic-wave dispersion relation.

#### 19.7.1

##### 19.7.1 Cosmic Rays

cosmic-ray spectrum

Cosmic rays are the high-energy particles, primarily protons, that bombard Earth's magnetosphere from outer space. They range in energy from  $\sim 1$  MeV to  $\sim 3 \times 10^{11}$  GeV =  $0.3$  ZeV  $\sim 50$  J. (The highest cosmic-ray energy ever measured was  $\sim 50$  J. Thus, naturally occurring particle accelerators are far more impressive than their terrestrial counterparts, which can only reach  $\sim 10$  TeV =  $10^4$  GeV!) Most subrelativistic particles originate in the solar system. Their relativistic counterparts, up to energies  $\sim 100$  TeV, are believed to come mostly from interstellar space, where they are accelerated by expanding shock waves created by supernova explosions (cf. Sec. 17.6.3). The origin of the highest energy particles, greater than  $\sim 100$  TeV, is an intriguing mystery.

isotropy

The distribution of cosmic-ray arrival directions at Earth is inferred to be quite isotropic (to better than 1 part in  $10^4$  at an energy of 10 GeV). This is somewhat surprising, because their sources, both in and beyond the solar system, are believed to be distributed anisotropically, so the isotropy needs to be explained. Part of the reason for the isotropy is that the interplanetary and interstellar media are magnetized, and

7. The magnetotail is the region containing trailing field lines on the night side of Earth.

the particles gyrate around the magnetic field with the gyro (relativistic cyclotron) frequency  $\omega_G = eBc^2/\mathcal{E}$ , where  $\mathcal{E}$  is the (relativistic) particle energy including rest mass, and  $B$  is the magnetic field strength. The gyro (Larmor) radii of the non-relativistic particle orbits are typically small compared to the size of the solar system, and those of the relativistic particles are typically small compared to characteristic lengthscales in the interstellar medium. Therefore, this gyrational motion can effectively erase any azimuthal asymmetry around the field direction. However, this does not stop the particles from streaming away from their sources along the magnetic field, thereby producing anisotropy at Earth. So something else must be impeding this along-line flow, by scattering the particles and causing them to effectively diffuse along and across the field through interplanetary and interstellar space.

As we verify in Sec. 20.4, Coulomb collisions are quite ineffective (even if they were effective, they would cause huge cosmic-ray energy losses, in violation of observations). We therefore seek some means of changing a cosmic ray's momentum without altering its energy significantly. This is reminiscent of the scattering of electrons in metals, where it is phonons (elastic waves in the crystal lattice) that are responsible for much of the scattering. It turns out that in the interstellar medium, magnetosonic waves can play a role analogous to phonons and can scatter the cosmic rays. As an aid to understanding this phenomenon, we now derive the waves' dispersion relation.

### 19.7.2 Magnetosonic Dispersion Relation

19.7.2

Our procedure for deriving the dispersion relation (last paragraph of Sec. 7.2.1) should be familiar by now. We consider a uniform, isentropic, magnetized fluid at rest; we perform a linear perturbation and seek monochromatic plane-wave solutions varying as  $e^{i(\mathbf{k}\cdot\mathbf{x}-\omega t)}$ . We ignore gravity and dissipative processes (specifically, viscosity, thermal conductivity, and electrical resistivity), as well as gradients in the equilibrium, which can all be important in some circumstances.

It is convenient to use the velocity perturbation  $\delta\mathbf{v}$  as the independent variable. The perturbed and linearized equation of motion (19.10) then takes the form

$$-i\rho\omega\delta\mathbf{v} = -iC^2\mathbf{k}\delta\rho + \frac{(i\mathbf{k} \times \delta\mathbf{B}) \times \mathbf{B}}{\mu_0}. \quad (19.70)$$

Here  $C$  is the sound speed [ $C^2 = (\partial P/\partial\rho)_s = \gamma P/\rho$ , not to be confused with the speed of light  $c$ ], and  $\delta P = C^2\delta\rho$  is the Eulerian pressure perturbation for our homogeneous equilibrium.<sup>8</sup> (Note that  $\nabla P = \nabla\rho = 0$ , so Eulerian and Lagrangian perturbations are the same.) The perturbed equation of mass conservation,  $\partial\rho/\partial t + \nabla \cdot (\rho\mathbf{v}) = 0$ , becomes

$$\omega\delta\rho = \rho\mathbf{k} \cdot \delta\mathbf{v}, \quad (19.71)$$

8. Note that we are assuming that (i) the equilibrium pressure tensor is isotropic and (ii) the perturbations to the pressure are also isotropic. This is unlikely to be the case for a collisionless plasma, so our treatment there must be modified. See Sec. 20.6.2 and Ex. 21.1.

and the MHD law of magnetic-field transport with dissipation ignored,  $\partial \mathbf{B} / \partial t = \nabla \times (\mathbf{v} \times \mathbf{B})$ , becomes

$$\omega \delta \mathbf{B} = -\mathbf{k} \times (\delta \mathbf{v} \times \mathbf{B}). \quad (19.72)$$

#### Alfvén velocity

We introduce the Alfvén velocity

$$\mathbf{a} \equiv \frac{\mathbf{B}}{(\mu_0 \rho)^{1/2}}, \quad (19.73)$$

and insert  $\delta \rho$  [Eq. (19.71)] and  $\delta \mathbf{B}$  [Eq. (19.72)] into Eq. (19.70) to obtain

#### eigenequation for magnetosonic waves

$$\{\mathbf{k} \times [\mathbf{k} \times (\delta \mathbf{v} \times \mathbf{a})]\} \times \mathbf{a} + C^2(\mathbf{k} \cdot \delta \mathbf{v})\mathbf{k} = \omega^2 \delta \mathbf{v}. \quad (19.74)$$

Equation (19.74) is an eigenequation for the wave's squared frequency  $\omega^2$  and eigendirection  $\delta \mathbf{v}$ . The straightforward way to solve it is to rewrite it in the standard matrix form  $M_{ij} \delta v_j = \omega^2 \delta v_i$  and then use standard matrix (determinant) methods. It is quicker, however, to seek the three eigendirections  $\delta \mathbf{v}$  and eigenfrequencies  $\omega$  one by one, by projection along preferred directions.

#### Alfvén mode and its dispersion relation

We first seek a solution to Eq. (19.74) for which  $\delta \mathbf{v}$  is orthogonal to the plane formed by the unperturbed magnetic field and the wave vector,  $\delta \mathbf{v} = \mathbf{a} \times \mathbf{k}$  up to a multiplicative constant. Inserting this  $\delta \mathbf{v}$  into Eq. (19.74), we obtain the dispersion relation

$$\omega = \pm \mathbf{a} \cdot \mathbf{k}; \quad \frac{\omega}{k} = \pm a \cos \theta, \quad (19.75)$$

where  $\theta$  is the angle between  $\mathbf{k}$  and the unperturbed field, and  $a \equiv |\mathbf{a}| = B/(\mu_0 \rho)^{1/2}$  is the Alfvén speed. This type of wave is known as the *intermediate magnetosonic mode* and also as the *Alfvén mode*. Its phase speed  $\omega/k = a \cos \theta$  is plotted as the larger figure-8 curve in Fig. 19.14. The velocity and magnetic perturbations  $\delta \mathbf{v}$  and  $\delta \mathbf{B}$  are both along the direction  $\mathbf{a} \times \mathbf{k}$ , so the Alfvén wave is fully transverse. There is no compression ( $\delta \rho = 0$ ), which accounts for the absence of the sound speed  $C$  in the dispersion relation. This Alfvén mode has a simple physical interpretation in the limiting case when  $\mathbf{k}$  is parallel to  $\mathbf{B}$ . We can think of the magnetic field lines as strings with tension  $B^2/\mu_0$  and inertia  $\rho$ , which are plucked transversely. Their transverse oscillations then propagate with speed  $\sqrt{\text{tension}/\text{inertia}} = B/\sqrt{\mu_0 \rho} = a$ . For details and delicacies, see Ex. 21.8.

#### Alfvén-mode properties

The dispersion relations for the other two modes can be deduced by projecting the eigenequation (19.74) successively along  $\mathbf{k}$  and along  $\mathbf{a}$  to obtain two scalar equations:

$$\begin{aligned} k^2(\mathbf{k} \cdot \mathbf{a})(\mathbf{a} \cdot \delta \mathbf{v}) &= [(a^2 + C^2)k^2 - \omega^2](\mathbf{k} \cdot \delta \mathbf{v}), \\ C^2(\mathbf{k} \cdot \mathbf{a})(\mathbf{k} \cdot \delta \mathbf{v}) &= \omega^2(\mathbf{a} \cdot \delta \mathbf{v}). \end{aligned} \quad (19.76)$$

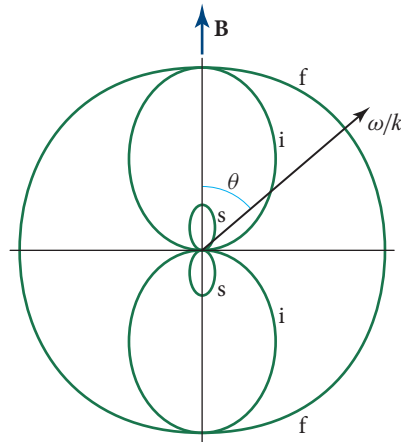


**FIGURE 19.14** Phase-velocity surfaces for the three types of magnetosonic modes: fast (f), intermediate (i), and slow (s). The three curves are polar plots of the wave phase velocity  $\omega/k$  in units of the Alfvén speed  $a = B/\sqrt{\mu_0\rho}$ . In the particular example shown, the sound speed  $C$  is half the Alfvén speed.

Combining these equations, we obtain the dispersion relation

$$\left(\frac{\omega}{k}\right)^2 = \frac{1}{2}(a^2 + C^2) \left[ 1 \pm \left( 1 - \frac{4C^2 a^2 \cos^2 \theta}{(a^2 + C^2)^2} \right)^{1/2} \right]. \quad (19.77)$$

dispersion relation for fast (+) and slow (−) magnetosonic modes

(By inserting this dispersion relation, with the upper or lower sign, back into Eqs. (19.76), we can deduce the mode's eigendirection  $\delta\mathbf{v}$ .) This dispersion relation tells us that  $\omega^2$  is positive, so no unstable modes exist, which seems reasonable, as there is no source of free energy. (The same is true, of course, for the Alfvén mode.)

These waves are compressive, with the gas being moved by a combination of gas pressure and magnetic pressure and tension. The modes can be seen to be non-dispersive, which is also to be expected, as we have introduced neither a characteristic timescale nor a characteristic length into the problem.

The mode with the plus signs in Eq. (19.77) is called the *fast magnetosonic mode*; its phase speed is depicted by the outer, quasi-circular curve in Fig. 19.14. A good approximation to its phase speed when  $a \gg C$  or  $a \ll C$  is  $\omega/k \simeq \pm(a^2 + C^2)^{1/2}$ . When propagating perpendicularly to  $\mathbf{B}$ , the fast mode can be regarded as simply a longitudinal sound wave in which the gas pressure is augmented by the magnetic pressure  $B^2/(2\mu_0)$  (adopting a specific-heat ratio  $\gamma$  for the magnetic field of 2, as  $B \propto \rho$  and so  $P_{\text{mag}} \propto \rho^2$  under perpendicular compression).

fast magnetosonic-mode properties

The mode with the minus signs in Eq. (19.77) is called the *slow magnetosonic mode*. Its phase speed (depicted by the inner figure-8 curve in Fig. 19.14) can be approximated by  $\omega/k = \pm aC \cos \theta / (a^2 + C^2)^{1/2}$  when  $a \gg C$  or  $a \ll C$ . Note that

slow magnetosonic-mode properties

slow mode—like the intermediate mode but unlike the fast mode—is incapable of propagating perpendicularly to the unperturbed magnetic field; see Fig. 19.14. In the limit of vanishing Alfvén speed or vanishing sound speed, the slow mode ceases to exist for all directions of propagation.

In Chap. 21, we will discover that MHD is a good approximation to the behavior of plasmas only at frequencies below the “ion cyclotron frequency,” which is a rather low frequency. For this reason, magnetosonic modes are usually regarded as low-frequency modes.

### 19.7.3

### 19.7.3 Scattering of Cosmic Rays by Alfvén Waves

mechanism for Alfvén waves to scatter cosmic-ray particles

Now let us return to the issue of cosmic-ray propagation, which motivated our investigation of magnetosonic modes. Let us consider 100-GeV particles in the interstellar medium. The electron (and ion, mostly proton) density and magnetic field strength are typically  $n \sim -3 \times 10^4 \text{ m}^{-3}$  and  $B \sim 300 \text{ pT}$ . The Alfvén speed is then  $a \sim 30 \text{ km s}^{-1}$ , much slower than the speeds of the cosmic rays. When analyzing cosmic-ray propagation, a magnetosonic wave can therefore be treated as essentially a magnetostatic perturbation. A relativistic cosmic ray of energy  $\mathcal{E}$  has a gyro (relativistic Larmor) radius of  $r_G = \mathcal{E}/eBc$ , in this case  $\sim 3 \times 10^{12} \text{ m}$ . Cosmic rays will be unaffected by waves with wavelength either much greater than or much less than  $r_G$ . However, magnetosonic waves (especially Alfvén waves, which are responsible for most of the scattering), with wavelength matched to the gyro radius, will be able to change the particle’s *pitch angle*  $\alpha$  (the angle its momentum makes with the mean magnetic field direction). See Sec. 23.4.1 for some details. If the Alfvén waves in this wavelength range have rms dimensionless amplitude  $\delta B/B \ll 1$ , then the particle’s pitch angle will change by an amount  $\delta\alpha \sim \delta B/B$  for every wavelength. Now, if the wave spectrum is broadband, individual waves can be treated as uncorrelated, so the particle pitch angle changes stochastically. In other words, the particle diffuses in pitch angle. The effective diffusion coefficient is

$$D_\alpha \sim \left( \frac{\delta B}{B} \right)^2 \omega_G, \quad (19.78)$$

where  $\omega_G = c/r_G$  is the gyro frequency (relativistic analog of cyclotron frequency  $\omega_c$ ). The particle is therefore scattered by roughly a radian in pitch angle every time it traverses a distance  $\ell \sim (B/\delta B)^2 r_G$ . This is effectively the particle’s collisional mean free path. Associated with this mean free path is a spatial diffusion coefficient

$$D_x \sim \frac{\ell c}{3}. \quad (19.79)$$

It is thought that  $\delta B/B \sim 10^{-1}$  in the relevant wavelength range in the interstellar medium. An estimate of the collision mean free path is then  $\ell(100 \text{ GeV}) \sim 10^{14} \text{ m}$ . Now, the thickness of our galaxy’s interstellar disk of gas is roughly  $L \sim 3 \times 10^{18} \text{ m} \sim 10^4 \ell$ . Therefore, an estimate of the cosmic-ray anisotropy is

estimated and measured cosmic-ray anisotropy

$\sim \ell/L \sim 3 \times 10^{-5}$ , roughly compatible with the measurements. Although this discussion is an oversimplification, it does demonstrate that the cosmic rays in the interplanetary, interstellar, and intergalactic media can be scattered efficiently by magnetosonic waves. This allows the particle transport to be impeded without much loss of energy, so that the theory of cosmic-ray acceleration (Ex. 23.12) and scattering (this section) together can account for the particle fluxes observed as a function of energy and direction at Earth.

A good question to ask at this point is “Where do the Alfvén waves come from?” The answer turns out to be that they are maintained as part of a turbulence spectrum and created by the cosmic rays themselves through the growth of plasma instabilities. To proceed further and give a more quantitative description of this interaction, we must go beyond a purely fluid description and explore the motions of individual particles. This is where we shall turn in the next few chapters, culminating with a return to the interaction of cosmic rays with Alfvén waves in Sec. 23.4.1.

### **Bibliographic Note**

For intuitive insight into magnetohydrodynamics, we recommend Shercliff (1965).

For textbook introductions to magnetohydrodynamics, we recommend the relevant chapters of Landau, Pitaevskii, and Lifshitz (1979), Schmidt (1979), Boyd and Sanderson (2003), and Bellan (2006). For far greater detail, we recommend a textbook that deals solely with magnetohydrodynamics: Goedbloed and Poedts (2004) and its advanced supplement Goedbloed, Keppens, and Poedts (2010). For a very readable treatment from the viewpoint of an engineer, with applications to engineering and metallurgy, see Davidson (2001).

For the theory of MHD instabilities and applications to magnetic confinement, see the above references, and also Bateman (1978) and the collection of early papers edited by Jeffrey and Taniuti (1966). For applications to astrophysics and space physics, see Parker (1979), Parks (2004), and Kulsrud (2005).

## NAME INDEX

---

Page numbers for entries in boxes are followed by “b,” those for epigraphs at the beginning of a chapter by “e,” those for figures by “f,” and those for notes by “n.”

- Alfvén, Hannes, 943e  
Appleton, Edward Victor, 1058n
- Bernstein, Ira B., 981, 1101  
Bogolyubov, Nikolai Nikolayevich, 1103  
Bohr, Niels, 1039n  
Born, Max, 1103
- Carlini, Francesco, 1165n
- Dyson, Freeman, 1111e
- Euler, Leonhard, 1178n
- Green, George, 1165n  
Green, Herbert S., 1103  
Greene, John M., 1101
- Hamilton, William Rowan, 1062  
Heaviside, Oliver, 995, 1033e, 1058n
- Jeans, James, 1071n  
Jeffreys, Harold, 1165n
- Kennelly, Arthur, 995, 1058e  
Kirkwood, John, 1103  
Kruskal, Martin, 1101
- Landau, Lev Davidovich, 1080  
Langmuir, Irving, 1044n, 1069e  
Leibniz, Gottfried Wilhelm, 1178n  
Liouville, Joseph, 1165n
- Maupertuis, Pierre Louis, 1178n
- Nyquist, Harry, 1091
- Penrose, Oliver, 1091
- Sakharov, Andrei Dmitrievich, 959n  
Spitzer, Lyman, 997e
- Taam, Igor Yevgenyevich, 959n
- Vlasov, Anatoly Alexandrovich, 1071n
- Yvon, Jacques, 1103

© Copyright Princeton University Press. No part of this book may be distributed, posted, or reproduced in any form by digital or mechanical means without prior written permission of the publisher.

For general queries contact [webmaster@press.princeton.edu](mailto:webmaster@press.princeton.edu).

## SUBJECT INDEX

Second and third level entries are not ordered alphabetically. Instead, the most important or general entries come first, followed by less important or less general ones, with specific applications last.

Page numbers for entries in boxes are followed by “b,” those for epigraphs at the beginning of a chapter by “e,” those for figures by “f,” for notes by “n,” and for tables by “t.”

- $\mathbf{E} \times \mathbf{B}$  drift, 1025, 1026f, 1039
- ⊖-pinch for plasma confinement, 961f, 962–963, 971
  - stability of, 978–979
- ⊖-pinch, toroidal, for plasma confinement, 978
  - flute instability of, 978–979, 978f
  
- Abbé condition, 1180n
- absorption of radiation, 1017, 1054, 1057, 1126–1130
- accretion disk around spinning black hole, 969
- action principles
  - for rays in geometric optics, 1178–1180
  - for eigenfrequencies of normal modes, 980–981
- adiabatic index
  - in plasma: anisotropic, 1020–1024
- adiabatic invariants
  - accuracy of, 1030
  - failure of, 1030
  - for charged particle in magnetic field, 1028–1030
  - wave action of a classical wave, 1172–1173
- Alcator C-Mod, 963
- Alfvén waves, 990–991, 1053f, 1161
  - two-fluid analysis of, 1055–1058
  - dispersion relation of, 990, 1161
  - phase velocity of, 990, 1161
  - group velocity of, 1162f, 1163
  - relativistic corrections for, 1055–1056
  - as plasma-laden, plucked magnetic field lines, 990, 1056–1057
  - in magnetosphere, 1177f
  - in solar wind, 970–971
    - generated near shock fronts, 1146f
    - interaction with cosmic rays. *See* cosmic rays
- angular momentum
  - in fluid mechanics, 1151, 1152
- angular momentum conservation
  - in circulating water, 1151–1152
- Appleton-Hartree dispersion relation, 1059–1060
- atomic bomb, 1009
  
- BBGKY hierarchy of kinetic equations, 1103–1106, 1109
- BGK waves in a plasma, 1100–1101
- bird flight
  - wingtip vortices, 1154f
- black holes
  - accretion of gas onto, 969
- bosons, 1187
- bow shock around Earth, 957, 1090, 1146–1147, 1146f
- bremsstrahlung, 1009, 1017
- Brillouin scattering, 1142
- bump-in-tail instability, 1136–1137, 1138–1139
- bunching of bosons, 1117
  
- Cerenkov emission of plasmons by fast electrons in a plasma, 1127–1129, 1131, 1133, 1138
- CGL equations of state, 1024
- chaos in dynamical systems
  - example of, 1030

- charge density
  - as integral over plasma distribution function, 1072
- charged-particle motion in electromagnetic field, 1024–1032
- chemical reactions, including nuclear and particle examples
  - electron-positron pair formation, 1001
  - ionization of hydrogen: Saha equation, 998–1000
  - controlled thermonuclear fusion, 959–960, 1141b
- circulation, 1154
- climate change, 958
- closure relation, in plasma kinetic theory, 1074, 1105
- CMA diagram for waves in cold, magnetized plasma, 1062–1065, 1064f
- collective effects in plasmas, 943, 1003–1006, 1016, 1020, 1070, 1146
- collisionless shocks, 1145–1147
- commutator
  - of two vector fields, 1155n
- conductivity, electrical,  $\kappa_e$ 
  - in plasmas with Coulomb collisions, 1015, 1018
  - in magnetized plasma, tensorial, 1022–1023, 1036
- contact discontinuity, 953
- controlled fusion. *See* fusion, controlled thermonuclear
- Coriolis acceleration, 1155
- correlation functions
  - for many-particle system, 1104–1106
  - two-point and three-point, 1104–1106
- cosmic rays
  - spectrum of, 988
  - ultra-high-energy, 1024
  - anisotropy of arrival directions, 992–993
  - acceleration of in strong shock fronts, 1147–1148
  - interaction with Alfvén waves, 992–993, 1138–1139
    - Cerenkov emission of Alfvén waves by, 1138–1139
    - observational evidence for scattering of, 989
    - scattering of, by Alfvén waves, 992–993, 1138–1139
- Coulomb correction to pressure in plasma, 1108
- Coulomb logarithm, 1008–1009
- Coulomb scattering
  - Rutherford scattering analysis, 1006–1007
  - Fokker-Planck analysis of, 1013–1015
  - deflection times and frequencies, 1008
  - energy equilibration times, 1010–1012, 1002t
- Cowling's theorem, for dynamos, 984
- cruise-control system for automobiles, 1097–1098
- current density
  - as integral over plasma distribution function, 1072
- curvature drift, 1026, 1027f
- cutoff, in wave propagation, 1049–1050, 1050f
- cyclotron frequencies, 1019, 1002t
  - relativistic, 1024
- Debye length, 1002t, 1004
- Debye number, 1002t, 1004
- Debye shielding, 1003–1004
- decay time for magnetic field, in MHD, 949, 950t
- degeneracy, of gas, 1000, 1002
- density of states (modes)
  - for free particles, 1186–1188
- derivatives of scalars, vectors, and tensors
  - Lie derivative, 1155n
- dielectric tensor, 1036
  - in cold, magnetized plasma, 1051–1052
- diffusion coefficient
  - for electrons interacting with electrostatic waves in plasma, 1118–1119, 1123
  - for magnetic field, in MHD, 948
- diffusion equation
  - for magnetic field, in MHD, 948
  - in nonlinear plasma physics, 1118–1119, 1135, 1148
- dispersion relation, 1159. *See also under* geometric optics
  - as Hamiltonian for rays, 1168, 1174
- distribution function
  - mean occupation number, 1185–1188. *See also* occupation number, mean
  - number density in phase space, 1184
  - $N$ -particle, 1102–1103
  - for particles in a plasma, 1071, 1185–1186
  - $N$ -particle, 1102–1103
- drift velocities
  - for charged particles in electromagnetic field, 1025–1027
  - for electron and ion fluids, 1038–1039
- drift waves, 1067–1068
- dynamos, 984–988
- eikonal approximation. *See* geometric optics
- electric charge. *See* charge density
- electromagnetic field. *See also* electromagnetic waves;
  - Maxwell's equations
  - electric displacement vector, 1036
- electromagnetic waves
  - in anisotropic, linear dielectric medium, 1035–1037
  - wave equation and dispersion relation, 1037
  - in cold plasma, 1035–1068
- electron motion in electromagnetic field, 1024–1032
- electrostatic waves. *See also* Langmuir waves; ion-acoustic waves; Landau damping
  - dispersion relation for, 1083–1084
  - for weakly damped or growing modes, 1085–1086
  - kinetic-theory analysis of, 1077–1079
  - stability analysis of, 1090–1092, 1095–1098
  - quasilinear theory of, 1113–1135
  - nonlinear: BGK waves, 1100–1101

- emission  
 spontaneous  
 of plasmons, in a plasma, 1126–1128  
 stimulated  
 of plasmons, in a plasma, 1134
- energy density,  $U$   
 deduced from lagrangian, 1172  
 for prototypical wave equation, 1172
- energy flux, Newtonian,  $F$   
 deduced from lagrangian, 1172  
 for prototypical wave equation, 1172
- energy principle for perturbations of magnetostatic equilibria, 980–982
- Eulerian perturbations, 971–972
- extraordinary waves  
 in a cold, magnetized plasma, 1057–1058, 1060, 1063, 1064f
- Faraday rotation, 1053–1054, 1060–1061
- feedback-control system, 1093b  
 stability analysis of, 1093b–1095b, 1098
- Fermat's principle, 1178  
 for dispersionless waves, 1179–1180  
 and Feynman sum over paths, 1179
- fermions, 1187
- Ferraro's law of isorotation for magnetosphere, 970
- flexural waves on a beam or rod, 1160, 1162f, 1163, 1175–1176
- fluid flows  
 barotropic, inviscid, 1155–1157
- flute instability for toroidal  $\ominus$ -pinch, 978–979, 978f
- Fokker-Planck equation  
 for Coulomb collisions, 1013–1016, 1032  
 for electrons interacting with plasmons, 1123, 1130–1131
- force-free magnetic field, 964
- Fourier transform, conventions for  
 in plasma physics, 1115
- fusion, controlled thermonuclear, 959–964, 999f, 1001, 1002t, 1140–1142  
 motivation for, 958–959  
 Lawson criterion for, 960  
 d, t fusion reaction, 959  
 magnetic confinement for, 960–964  
 laser fusion, 1140–1142
- gain margin, for stability of control system, 1095b, 1098
- galaxies  
 dark matter in, 1076n
- gas, hydrogen, 999f
- gas discharge, in laboratory, 999f, 1001, 1002t
- geometric optics, 1164–1182. *See also* Fermat's principle  
 as two-lengthscale expansion for a wave, 1164, 1166, 1167  
 limitations (failure) of, 1176–1178  
 for a completely general wave, 1173–1175  
 for prototypical wave equation, 1165–1173  
 eikonal approximation, 1166  
 connection to quantum theory, 1169–1172  
 rays and Hamilton's equations for them, 1168  
 dispersion relation as Hamiltonian, 1168, 1174  
 amplitude and its propagation, 1166, 1168, 1171–1172, 1175  
 phase and its propagation, 1166, 1169, 1174  
 angular frequency and wave vector, 1166  
 energy density,  $U$ , 1166  
 energy flux,  $F$ , 1166  
 quanta, 1170  
 conservation of, 1171, 1172, 1175  
 Hamiltonian, energy, momentum, number density, and flux of, 1170  
 eikonal equation (Hamilton-Jacobi equation), 1169  
 for dispersionless waves in time-independent medium  
 index of refraction, 1179  
 ray equation, 1180  
 Fermat's principle: rays have extremal time, 1179  
 Snell's law, 1180, 1181f
- examples  
 light propagating through lens, 1177f  
 light rays in an optical fiber, 1181–1182  
 flexural waves in a tapering rod, 1175–1176  
 spherical sound waves, 1175, 1176  
 Alfvén waves in Earth's magnetosphere, 1177f
- global warming, 958
- globular star cluster, energy equilibration time for, 1012–1013. *See also* stellar dynamics
- gradient drift, 1027, 1027f
- gravitational drift of charged particle in magnetic field, 1026
- gravitational waves  
 dispersion relation for, 1161
- gravity waves on water, 1160, 1162f, 1163  
 deep water, 1160, 1162f, 1163
- greenhouse effect, 958
- group velocity, 1162
- guiding-center approximation for charged-particle motion, 1025–1030, 1055
- gyro frequencies. *See* cyclotron frequencies
- Hamilton-Jacobi equation, 1169, 1182
- Hamilton's equations  
 for rays in geometric optics, 1168–1170, 1174  
 for plasmons, 1124
- Hamilton's principal function, 1169, 1182

- Hartmann flow, 965–969  
Hartmann number, 968  
helicity  
    hydrodynamic, 985  
    magnetic, 965  
hydrogen gas. *See* gas, hydrogen  
hydromagnetic flows, 965–971
- index of refraction, 1179  
    for optical fiber, 1181  
    for plasma waves, 1052, 1057, 1058f  
intergalactic medium, 999f, 1002, 1002t  
interstellar medium, 950t, 989, 992, 999f, 1001, 1002t, 1012, 1060–1061, 1138–1139, 1146–1147  
ion-acoustic waves. *See also* electrostatic waves; plasmons  
    in two-fluid formalism, 1046–1050  
    in kinetic theory, 1088–1090  
    Landau damping of, 1088  
    nonlinear interaction with Langmuir waves, 1132–1135  
    solitons, 1142–1146  
ionosphere, 999f, 1001, 1002t, 1059  
    radio waves in, 1058–1062  
ITER (International Thermonuclear Experimental Reactor), 963
- Jeans’ theorem, 1074–1077, 1100  
JET (Joint European Torus), 963  
junction conditions  
    MHD, 953–956  
Jupiter, 1100
- KDP nonlinear crystal, 1141b  
kink instability, of magnetostatic equilibria, 977–978  
Korteweg–de Vries equation and soliton solutions, 1048–1049
- lagrangian density  
    energy density and flux in terms of, 1172  
    for prototypical wave equation, 1172  
Lagrangian perturbations, 971–972  
Landau contour, 1082f, 1083  
Landau damping  
    physics of: particle surfing, 1046, 1069–1070, 1098–1099  
    for ion-acoustic waves, 1088–1090  
    for Langmuir waves, 1086–1088  
    in quantum language, 1127–1129  
Langmuir waves. *See also* electrostatic waves; plasmons  
    in two-fluid formalism, 1044–1047  
    in kinetic theory, 1086–1088, 1090  
    in quasilinear theory, 1115–1123  
    summary of, in one dimension, 1120  
    evolution of electron distribution, 1118–1120  
    evolution of wave spectral density, 1118  
    in three dimensions, 1122–1123  
    Landau damping of, 1086–1088, 1098–1099  
    particle trapping in, 1098–1100  
    nonlinear interaction with ion-acoustic waves, 1132–1135  
Laplace transform, 1081, 1084  
    used to evolve initial data, 1081  
Larmor radius, 1019, 1002t  
Lawson criterion for controlled fusion, 960  
least action, principle of, 1178, 1178n  
left modes, for plasma electromagnetic waves parallel to magnetic field, 1052–1056  
Lenz’s law, 945  
Lie derivative, 1155n  
Lorentz contraction of volume, 1184
- magnetic bottle, 1028, 1029f  
magnetic confinement of plasma, for controlled fusion, 960–964  
magnetic field diffusion in MHD, 948–950, 950t, 956  
magnetic field interaction with vorticity, 957–958, 958f  
magnetic field-line reconnection, 950, 986–988, 987f  
magnetic force density on fluid, in MHD, 951–952  
magnetic Reynolds number, 950, 950t  
magnetization  
    in magnetized plasma, 1039  
magnetohydrodynamics (MHD), 943–993  
    conditions for validity, 1020  
    fundamental equations of  
        electric field, charge, and current density in terms of magnetic field, 947–948  
        magnetic-field evolution equation, 948  
        freezing-in of magnetic field, 948  
        magnetic field diffusion, 948  
        fluid equation of motion, 951  
        magnetic force density on fluid, 951–952  
        boundary conditions and junction conditions, 953–956  
        momentum conservation, 951  
        energy conservation, 952  
        entropy evolution, 953  
        Ohm’s law, 947  
    generalizations of, 1020–1022  
magnetoionic theory, for radio waves in atmosphere, 1058–1062  
magnetosonic waves, 988–992  
    Alfvén waves (intermediate magnetosonic mode), 990–991, 1053f, 1161–1162. *See also* Alfvén waves  
    fast magnetosonic mode, 990–992  
    slow magnetosonic mode, 990–992

- magnetosphere, 999f, 1001, 1002t  
rotating, 969–970  
Alfvén waves in, 1177f  
interaction of solar wind with Earth's, 950, 957, 987–988, 1090, 1146–1147, 1146f
- magnetostatic equilibria, 958–965, 971, 1030–1031  
equations of, 960, 962  
perturbations and stability of, 971–984  
dynamical equation, 973  
boundary conditions, 974  
energy principle, 980–982  
virial theorems, 982–984
- Maxwell's equations  
in terms of electric and magnetic fields, 946  
in linear, polarizable (dielectric) medium, 1036
- MHD electromagnetic brake, 966, 967f  
MHD electromagnetic pump, 966–968, 967f  
MHD flow meter, 966, 967f  
MHD power generator, 966, 967f  
mirror machine for confining plasma, 963, 1030–1031  
mirror point for particle motion in magnetic field, 1027f, 1028–1029, 1029f
- moments, method of: applications  
constructing fluid models from kinetic theory, 1074
- momentum space, 1183, 1184f
- multiplicity for particle's spin states,  $g_s$ , 1187
- National Ignition Facility, 1141b
- neutrinos  
chirality of, 1187n  
spin-state multiplicity, 1187
- neutron stars  
structures of, 1153  
magnetospheres of, 969–970
- normal modes  
Sturm-Liouville, 974–975  
of magnetostatic equilibria, 975–976, 980–981
- nuclear reactions. *See* chemical reactions, including nuclear and particle
- Nyquist diagram and method for analyzing stability, 1091–1098, 1092f
- occupation number, mean  
defined, 1187  
ranges, for fermions, bosons, distinguishable particles, and classical waves, 1187–1188  
for plasmon modes in a plasma, 1123–1124
- Ohm's law. *See also* conductivity, electrical  
in magnetohydrodynamics, 946–947  
tensorial in magnetized plasmas, 1036
- Ohmic dissipation, 945, 949–950, 953, 957, 966, 987–988
- Onsager relation, 1018
- optical fiber  
light rays in, 1181
- ordinary waves  
in a cold, magnetized plasma, 1057–1058, 1060, 1063, 1064f
- pairs, electron-positron  
thermal equilibrium of, 1001  
temperature-density boundary for, 999f
- parametric amplification, 1140–1142
- parametric instability, 1140–1141
- Parseval's theorem, 1116–1117
- particle conservation law  
in plasma, 1071
- particle kinetics in phase space, 1183–1184
- path integrals in quantum mechanics, 1178–1179
- Penning trap, 1031–1032
- Penrose stability criterion for electrostatic waves, 1097
- perfect MHD, 950
- phase margin, for stability of control system, 1098
- phase space, 1183–1184
- phase velocity, 1159
- phonons  
momentum and energy of, 1170
- pitch angle, 1028
- plasma electromagnetic waves  
validity of fluid approximation for, 1020  
in unmagnetized plasma, 1042–1044, 1050  
in magnetized plasma, parallel to magnetic field: left and right modes, 1052–1066
- plasma frequency, 1005, 1002t, 1041
- plasma oscillations  
elementary analysis of, 1005  
in two-fluid formalism, 1041–1042  
in moving reference frame, 1065  
two-stream instability for, 1065–1067
- plasma waves  
in an unmagnetized, cold plasma, 1040–1044. *See also* plasma electromagnetic waves; plasma oscillations  
in a magnetized, cold plasma, 1050–1065. *See also* Alfvén waves; ordinary waves; extraordinary waves; magnetosonic waves; plasma oscillations; whistler wave in plasma  
in an unmagnetized, warm plasma, 1044–1050. *See also* ion-acoustic waves; Langmuir waves
- plasmas. *See also* plasma waves; plasmons  
summary in density-temperature plane, 999f  
summary of parameter values for, 1002t  
electron correlations (antibunching) in, 1106  
electron-positron pair production in, 1001

- plasmas (*continued*)  
ionization of, 999–1000  
degeneracy of, 1000, 1002  
examples of, 999f, 1001–1002, 1002t  
relativistic, 1000
- plasmons. *See also* ion-acoustic waves; Langmuir waves;  
quasilinear theory in plasma physics  
mean occupation number for, 1124  
master equation for evolution of, 1126  
fundamental emission rates, 1127, 1133–1134  
interaction with electrons, 1124–1131  
nonlinear interaction with each other, 1132–1135
- Poiseuille flow (confined laminar, viscous flow)  
between two plates with MHD magnetic field, 965–969
- Poisson's equation, 1003, 1078
- polarization of charge distribution  
in a linear dielectric medium, 1036  
in a plasma, 1035–1036
- pressure ratio  $\beta$  in MHD, 959
- pulsar. *See also* neutron stars  
radio waves from, 1060–1061
- quasars, 969, 995
- quasilinear theory in plasma physics. *See also* ion-acoustic waves; Langmuir waves  
in classical language, 1113–1123  
in three dimensions, 1122–1123  
in quantum language, 1123–1135
- radiative processes  
bremsstrahlung, 1009, 1017  
Raman scattering, 1140
- radio waves: AM, FM, and SW, 1060
- Raman scattering, stimulated, 1140
- random walk, 1007
- random-phase approximation, 1116–1117, 1137
- Rayleigh principle, 980. *See also* action principles
- refractive-index surface, 1062–1063, 1062f
- resonance conditions in wave-wave mixing, 1132
- rest frame, local, 1173
- Reynolds number  
magnetic, 950, 987
- right modes, for plasma electromagnetic waves parallel to magnetic field, 1052–1056
- Rutherford scattering, 1006–1007
- Saha equation for ionization equilibrium, 999–1000
- sausage instability, of magnetostatic equilibria, 977
- Schrödinger equation  
and Coulomb wave functions, 1009  
geometric optics for, 1181–1182
- Shapiro time delay, 1009
- shock waves (shock fronts) in a fluid, adiabatic  
bow shock in solar wind around Earth, 957, 1146–1147, 1146f  
acceleration of cosmic rays in, 1145–1148
- shock waves in a plasma, collisionless, 1145–1147, 1146f
- solar dynamo, 985–986
- solar wind, 970–971, 988, 999f, 1001, 1002t  
two-stream instability in, 1066–1067  
collisionless shocks in, 1146  
bow shock at interface with Earth, 957, 1090, 1146–1147, 1146f  
termination shock with interstellar medium, 1146–1147
- solitons  
in ion-acoustic waves in plasma, 1142–1146
- sound waves in a fluid  
dispersion relation, 1160  
phase velocity and group velocity, 1162  
propagating in a horizontal wind with shear, 1173  
quanta: phonons, 1170. *See also* phonons
- spectral energy density  $\mathcal{E}_k$ , in quasilinear theory of plasma waves, 1117
- spheromak, 964
- stellar dynamics. *See also under* galaxies  
Jeans' theorem in, 1076–1077  
equilibration time for stars in cluster, 1012–1013
- Sturm-Liouville equation and theory, 974–975, 980–981
- sun. *See also* solar dynamo; solar wind  
core of, 999f, 1001, 1002t  
disturbances on surface, 1035, 1065
- superfluid, rotating, 1153
- surfing of electrons and protons on electrostatic waves, 1046, 1069–1070, 1098–1099. *See also* Landau damping
- susceptibilities, dielectric  
linear, 1036
- thermoelectric transport coefficients, 1017–1018
- three-point correlation function, 1105
- three-wave mixing in plasmas  
driving term for, in Vlasov equation, 1114  
quasilinear theory of, 1132–1135
- tokamak, 963  
MHD stability of, 979
- transport coefficients. *See also* diffusion coefficient  
in plasmas, 1015–1018  
thermoelectric, 1017–1018
- two-fluid formalism, for plasma physics, 1037–1068  
fundamental equations, 1037–1038  
deduced from kinetic theory, 1073–1074
- two-lengthscale expansion  
bookkeeping parameter for, 1167b

- for geometric optics, 1164–1165, 1166–1167
- for quasi-linear theory in plasma physics, 1113–1114
- two-point correlation function, 1104–1107
  - for Coulomb corrections to pressure in a plasma, 1107–1108
  - for electron antibunching in a plasma, 1104–1107
- two-stream instability
  - in two-fluid formalism, 1065–1068
  - in kinetic theory, 1079–1080, 1137
- van Allen belts, 1028, 1029f
- virial theorems
  - for any system obeying momentum conservation, 982–984
  - for self-gravitating systems, 984
  - MHD application, 982, 984
- Vlasov equation, in plasma kinetic theory, 1071–1072
  - solution via Jeans' theorem, 1075
- volume in phase space, 1183
- vortex. *See also* vortex lines; vorticity
  - above a water drain, 1151
  - wingtip vortex, 1154f
  - tornado, 1151
- vortex cores, in superfluid, 1153
- vortex lines, 1153–1154, 1154f
  - frozen into fluid, for barotropic, inviscid flows, 1155–1157, 1157f
- vorticity, 1151–1152, 1152f
  - measured by a vane with orthogonal fins, 1151–1152
  - evolution equations for, 1153–1157
    - frozen into an inviscid, barotropic flow, 1155–1157
  - interaction with magnetic field, 957–958
  - delta-function: constant-angular-momentum flow, 1151–1152
- Voyager spacecraft, 1147
- water waves. *See* gravity waves on water; sound waves in a fluid
- wave equations
  - prototypical, 1165
    - lagrangian, energy density flux, and adiabatic invariant for, 1172–1173
  - algebratized, 1037
    - for electromagnetic waves. *See* electromagnetic waves
- wave packet, 1161–1163
  - Gaussian, 1163–1164
  - spreading of (dispersion), 1163–1164
- wave-normal surface, 1062–1063, 1062f, 1064f
- wave-wave mixing
  - in plasmas, 1132–1135
- waves, monochromatic in homogeneous medium. *See also* sound waves in a fluid; gravity waves on water; flexural waves on a beam or rod; gravitational waves; Alfvén waves
  - dispersion relation, 1159
  - group velocity, 1162
  - phase velocity, 1159
  - plane, 1159
- whistler wave in plasma, 1053f, 1054–1055, 1062f, 1146f
- winds, propagation of sound waves in, 1173
- wingtip vortices, 1154f
- WKB approximation, as example of eikonal approximation, 1165
- zero point energy, 1002
- Z-pinch for plasma confinement, 960–962, 961f
  - stability of, 975–978